

^{111}In -Labeled Dimeric Cyclic RGD Peptides as Integrin $\alpha_v\beta_3$ -Targeted Radiotracers for Breast Tumor Imaging

Diplomarbeit

vorgelegt von
Elena Tomaselli

zur Erlangung des akademischen Grades
Magister in Pharmazie

PURDUE
UNIVERSITY

University of Innsbruck, Austria
University of Purdue, USA



Supervisors: Univ.-Prof. Dr. Liu Shuang, Univ.-Prof. Dr. Striessnig Joerg

Collaborators: Univ.-Doz. Mag. Dr. Clemens Decristoforo

The following thesis was written under the supervision of Univ.-Prof. Dr. Liu Shuang at Purdue University, West Lafayette, Indiana, USA. The experiments took place in the Department of Human Health Sciences between July 15th 2013 and October 31st 2013.

Acknowledgment

This thesis research project was supported and funded by the Marshall Plan Foundation, Austria.

To Univ.-Prof.-Dr. Striessnig, who gave me the opportunity to do my thesis research abroad, trusted in my potential and supported my international ambitions.

To Univ.-Prof.-Dr. Liu, who gave me the chance to be part of his research, displayed great patience in answering all my questions, and quenched my thirst for knowledge. His generosity opened the doors for me to explore the fascinating world of research.

To Univ.-Doz. Mag. Dr. Decristoforo, for teaching me the fundamentals related to radiopharmaceutical science and for kindling my passion for nuclear pharmacy.

To Dr. Ji Shoundong, for teaching me all the necessary procedure in the lab, sharing his knowledge about nuclear medicine, and helping me understand the statistical analysis of the collected data.

To Purdue University, for giving me the chance to be a part of their wonderful institution.

To my family, for investing in my future, pushing me to reach farther and giving me the chance to receive an international education.

To the Muensterman family, for all their support and help during my stay in the United States of America.

To my boyfriend John Muensterman, for always standing at my side and for encouraging me to persevere when I thought I could not make it through.

**“He who has a reason to live can bear almost any how.”
Friedrich Nietzsche**

Kurzbeschreibung

Das Ziel dieser Diplomarbeit war die Evaluierung von $^{111}\text{In}(\text{DOTA-Galacto-RGD}_2)$ (DOTA = 1,4,7,10-tetraazacyclododecane-1,4,7,10-tetracetic acid, Galacto-RGD₂ = Glu[cyclo[Arg-Gly-Asp-D-Phe-Lys(SAA-PEG₂-(1,2,3-triazole)-1-yl-4-methylamide)]₂, SAA = 7-amino-L-glycero-L-galacto-2,6-anhydro-7-deoxyheptanamide, and PEG₂ = 3,6-dioxaoctanoic acid) und $^{111}\text{In}(\text{NOTA-Bz-Galacto-RGD}_2)$ (NOTA-Bz = 2-(p-thioureidobenzyl)-1,4,7-triazacyclononane-1,4,7-triacetic acid) als Radiotracer für die Visualisierung von $\alpha_v\beta_3$ Integrin in Brustkrebs.

DOTA-Galacto-RGD₂ und NOTA-Bz-Galacto-RGD₂ wurden mittels Konjugierung von Galacto-RGD₂ mit 1,4,7,10-tetraazacyclododecane-4,7,10-triacetic acid-1-acetate(N-hydroxysuccinimide) (DOTA-OSu) und 2-(p-thiocyanatobenzyl)-1,4,7-triazacyclononane-1,4,7-triacetic acid (SCN-Bz-NOTA) synthetisiert. DOTA-Galacto-RGD₂ and NOTA-Bz-Galacto-RGD₂ wurden zur Untersuchung ihrer Affinität zu $\alpha_v\beta_3$ Integrin in einem Verdrängungsassay mit ^{125}I -echistatin gebunden an U87MG Glioma Zellen evaluiert. Die Synthese von $^{111}\text{In}(\text{DOTA-Galacto-RGD}_2)$ and $^{111}\text{In}(\text{NOTA-Bz-Galacto-RGD}_2)$ war charakterisiert durch eine hohe radiochemische Reinheit (>95%) und die chemische Stabilität in Lösung war über >72 h nach der radioaktiven Markierung gegeben. $^{111}\text{In}(\text{DOTA-Galacto-RGD}_2)$ und $^{111}\text{In}(\text{NOTA-Bz-Galacto-RGD}_2)$ wurden bezüglich ihrer „Tumor-Targeting“ Fähigkeit und ihrer Bioverteilung evaluiert. Die Experimente wurden in athymischen Nacktmausmodellen durchgeführt, denen MDA-MB-435 humane Krebszellen injiziert wurden. Die Ergebnisse wurden mit denen von $^{111}\text{In}(\text{DOTA-3P-RGD}_2)$ (3P-RGD₂ = PEG₄-E[PEG₄-c(RGDfK)]₂; und PEG₄ = 15-amino-4,7,10,13-tetraoxapentadecanoic acid) verglichen. Es wurde festgestellt, dass die Aufnahme im Tumorgewebe (6.79 ± 0.98 , 6.56 ± 0.56 , 4.17 ± 0.61 and 1.09 ± 0.13 %ID/g nach 1, 4, 24 und 72 h p.i) fast gleich zur jenen von $^{111}\text{In}(\text{DOTA-3P-RGD}_2)$ (6.17 ± 1.65 , 5.94 ± 0.84 , 3.40 ± 0.50 und 0.99 ± 0.20 %ID/g, respectively) im gleichen

Tiermodell war. $^{111}\text{In}(\text{DOTA-Galacto-RGD}_2)$ zeigte eine schnellere Clearance aus dem Blut und aus den Muskeln als $^{111}\text{In}(\text{DOTA-3P-RGD}_2)$, was zur Folge hat, dass höhere Tumor/Blut und Tumor/Muskel Verhältnisse erreicht wurden. Hohe Aufnahme in der Leber führten allerdings zu einem niedrigerem Tumor/Leber Verhältnis im Vergleich zu $^{111}\text{In}(\text{DOTA-3P-RGD}_2)$. Kein signifikanter Unterschied wurde in der Aufnahme in der Lunge und im Tumor/Lunge Verhältnis festgestellt. Durch planare Gamma Kamera Aufnahmen konnten wir feststellen, dass $^{111}\text{In}(\text{DOTA-Galacto-RGD}_2)$, $^{111}\text{In}(\text{DOTA-3P-RGD}_2)$ und $^{111}\text{In}(\text{NOTA-Galacto-RGD}_2)$ als SPECT Radiotracer für die Visualisierung von $\alpha_v\beta_3$ integrin- Brustkrebs so wie potentielle Metastasen verwendet werden können.

Obwohl die planaren Aufnahmen von $^{111}\text{In}(\text{NOTA-Galacto-RGD}_2)$ eine Anreicherung des Radiotracers zeigen, sind die Ergebnisse aus der Biodistribution Studie für diesen Radiotracer noch nicht zufriedenstellend und bedürfen weiterer Optimierung.

Abstract

In this thesis work we evaluated $^{111}\text{In}(\text{DOTA-Galacto-RGD}_2)$ (DOTA = 1,4,7,10-tetraazacyclododecane-1,4,7,10-tetracetic acid, Galacto-RGD₂ = Glu[cyclo[Arg-Gly-Asp-D-Phe-Lys(SAA-PEG2-(1,2,3-triazole)-1-yl-4-methylamide)]]₂, SAA = 7-amino-L-glycero-L-galacto-2,6-anhydro-7-deoxyheptanamide, and PEG2 = 3,6-dioxaoctanoic acid) and $^{111}\text{In}(\text{NOTA-Bz-Galacto-RGD}_2)$ (NOTA-Bz = 2-(p-thioureidobenzyl)-1,4,7-triazacyclononane-1,4,7-triacetic acid) as $\alpha_v\beta_3$ integrin-targeted radiotracers for breast tumor imaging. DOTA-Galacto-RGD₂ and NOTA-Bz-Galacto-RGD₂ were prepared by conjugation of Galacto-RGD₂ with 1,4,7,10-tetraazacyclododecane-4,7,10-triacetic acid-1-acetate(N-hydroxysuccinimide) (DOTA-OSu) and 2-(p-thiocyanatobenzyl)-1,4,7-triazacyclononane-1,4,7-triacetic acid (SCN-Bz-NOTA), respectively. DOTA-Galacto-RGD₂ and NOTA-Bz-Galacto-RGD₂ were evaluated for their $\alpha_v\beta_3$ integrin binding affinity in a competitive displacement assay using ^{125}I -echistatin bound to U87MG glioma cells. The IC₅₀ were 27±2 and 24±4 nM for DOTA-Galacto-RGD₂ and NOTA-Bz-Galacto-RGD₂, respectively. $^{111}\text{In}(\text{DOTA-Galacto-RGD}_2)$ and $^{111}\text{In}(\text{NOTA-Bz-Galacto-RGD}_2)$ were prepared with high radiochemical purity (>95%), and remained stable in solution for >72 h post-labeling. $^{111}\text{In}(\text{DOTA-Galacto-RGD}_2)$ and $^{111}\text{In}(\text{NOTA-Bz-Galacto-RGD}_2)$ were evaluated for their tumor-targeting capability and biodistribution properties in athymic nude mice bearing MDA-MB-435 human breast tumor xenografts. The results were compared with those of $^{111}\text{In}(\text{DOTA-3P-RGD}_2)$ (3P-RGD₂ = PEG₄-E[PEG₄-c(RGDfK)]₂; and PEG₄ = 15-amino-4,7,10,13-tetraoxapentadecanoic acid). It was found that its tumor uptake (6.79 ± 0.98, 6.56 ± 0.56, 4.17 ± 0.61 and 1.09 ± 0.13 %ID/g at 1, 4, 24 and 72 h p.i., respectively) was almost identical to that of $^{111}\text{In}(\text{DOTA-3P-RGD}_2)$ (6.17 ± 1.65, 5.94 ± 0.84, 3.40 ± 0.50 and 0.99 ± 0.20 %ID/g, respectively) in the same animal model. $^{111}\text{In}(\text{DOTA-Galacto-RGD}_2)$ had a faster clearance from

blood and muscle than $^{111}\text{In}(\text{DOTA-3P-RGD}_2)$, leading to much higher tumor/blood and tumor/muscle ratios. However, its tumor/liver ratios are lower than those of $^{111}\text{In}(\text{DOTA-3P-RGD}_2)$ due to its higher liver uptake. There was no significant difference in their lung uptake and tumor/lung ratios. Planar imaging data suggest that both $^{111}\text{In}(\text{DOTA-Galacto-RGD}_2)$, $^{111}\text{In}(\text{DOTA-3P-RGD}_2)$ and $^{111}\text{In}(\text{NOTA-Galacto-RGD}_2)$ are all useful as SPECT radiotracers for imaging $\alpha_v\beta_3$ integrin-positive breast tumors and related metastases. Despite planar images of $^{111}\text{In}(\text{NOTA-Galacto-RGD}_2)$ were promising, its quantified tumor accumulation in the biodistribution study is significantly lower than the one of $^{111}\text{In}(\text{DOTA-Galacto-RGD}_2)$. This questions the suitability of $^{111}\text{In}(\text{NOTA-Galacto-RGD}_2)$ as a radiotracer for $\alpha_v\beta_3$ integrin-positive breast tumors and requires optimization in further research.

Table of contents

1. Introduction	1
1.1 Tumor Imaging in Nuclear Medicine	1
1.2 Integrins	5
1.2.1. Integrins in General	5
1.2.2. Integrin in Cancer	7
1.2.3. Integrin $\alpha_v\beta_3$ in Angiogenesis	9
1.2.4. Ligands for $\alpha_v\beta_3$	12
1.4. Radiopharmaceuticals	13
1.4.1. Radiolabeled peptides and their development	16
1.4.2. Radiolabeled peptides for integrin $\alpha_v\beta_3$	19
2. Materials and experimental procedure	23
3. Results	32
4. Discussion	43
5. Conclusion	46
6. Tables and Figures	48
7. Annex	52
8. References	60
9. List of Abbreviations	81
10. Curriculum Vitae	84

“A change of strategy in the world of cancer”

(Robert A. Gaten, Nature, Vol. 459, May 2009)

“Eradicating the large, diverse and adaptive populations found in most cancers presents a formidable challenge. One centimeter cubed of cancer contains about 10⁹ transformed cells and weighs about 1 gram, which means there are more cancer cells in 10 grams of tumor than there are people on Earth. Tumors are complex ecosystems: they include normal cells as well as regions of low blood flow and oxygen content where cancer cells are relatively protected from the effects of chemotherapy.”

“The typical goal in cancer therapy, similar to that of antimicrobial treatments, is killing as many tumor cells as possible under the assumption that this will, at best, cure the disease and, at worst, keep the patient alive for as long as possible. Indeed, for more than 50 years, oncologists have tried to find ways to administer ever-larger doses of ever-more cytotoxic therapy. But, just as invasive species consistently adapt to pesticides, regardless of concentration or cleverness of design, so too do cancerous cells adapt to therapies. Indeed, the parallels between cancerous cells and invasive species suggest that the principles for successful cancer therapy might lie not in the magic bullets of microbiology but in the evolutionary dynamics of applied ecology.”

“Even now, many oncologists agree in principle that therapeutic strategies aimed at controlling cancer could prove more effective than trying to cure it. But the idea of killing not the maximum number of tumor cells possible but the fewest necessary will be difficult for both physicians and patients to accept in practice.”

1. Introduction

1.1 Tumor Imaging in Nuclear Medicine

Several modalities to visualize tumors have been developed throughout the past decades. These include x-ray computed tomography (CT), magnetic resonance imaging (MRI), positron emission tomography (PET), single- photon emission computed tomography (SPECT) and ultrasound. Keeping track of the development of cancer and verifying the efficiency of the treatment is the primary purpose of any tumor imaging technique. CT and MRI can characterize a tumor by observing the changes in its volume. Nuclear medicine tomographic techniques such as PET and SPECT make it possible to target functional properties such as the micro-vascular characteristics of a tumor by tracking signaling molecules expressed on tumors and vessels involved in angiogenesis such as integrin receptors [2]. Other particular features of the tumor like its growth rate, receptor expression and metabolism could be successfully detected [110-112]. This explains why PET and SPECT have become the most important imaging modalities in nuclear medicine.

There are two different types of emission computed tomography that can detect the distribution of a radiolabeled molecule in the human or animal body. SPECT uses gamma-emitting radionuclides such as ^{99m}Tc , ^{123}I , ^{67}Ga , ^{111}In , while PET makes utilize of β^+ -emitting radionuclides such as ^{11}C , ^{13}N , ^{15}O , ^{18}F , ^{68}Ga . PET detects several pairs of gamma-rays, which are produced indirectly by a positron that is emitted from the radionuclide injected in the body. More precisely the system detects two 511-keV photons emitted in opposite directions after annihilation of a positron and an electron the emitted photons come from many position around the body axis of the patient. The multitude of collected data allows to create a reconstructed image which shows the activity in the desired area. In SPECT, the emission systems consist of a gamma-camera with one

to three NaI(Tl) detector heads for the acquisition and processing of data (Figure 1). The detector head rotates around the long axis of the patient at small angle increments (3° – 10°) for 180° or 360° angular sampling. The data is saved in the computer and used for later reconstruction of the images of the planes (slices) of interest. SPECT images are captured by a so called gamma camera which acquires multiple 2D images, so called projections, from many angles around the patient. Through a computer program, the images are reconstructed by using tomographic reconstruction algorithm, which provides final 3D image of the distribution of the radioactivity emitted by the radionuclide [117].

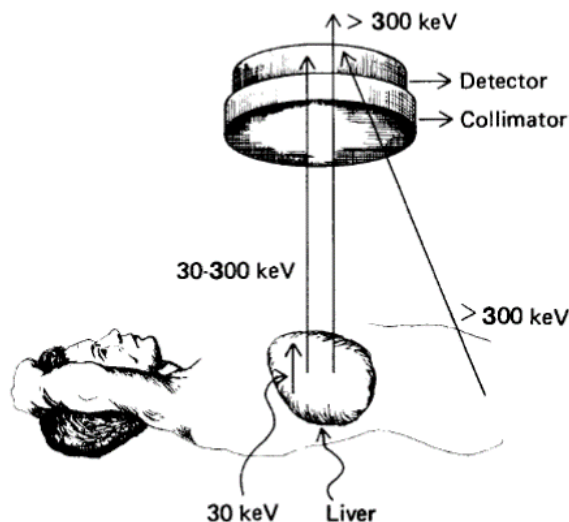


Figure 1- Photon interaction in the NaI(Tl) detector (Fundamentals of nuclear Pharmacy, Springer 5th edition, Gopal B. Saha, 2004)

This way, transverse, sagittal, and coronal images can be obtained from the collected data.

The SPECT scan requires a collimator to find the source of tracer accumulation and reconstruct the images. In fact, in the SPECT only one single γ -rays - instead of two like in the PET – are detected. This one photon can go in a single direction and needs therefore to be detected with a collimator. The downside of this system is that the presence of a collimator screens out most of the produced photons. As a consequence of this, the sensitivity of the SPECT scan is lower.

Despite this, the newest SPECT systems are able to capture the projection of radiotracers coming from the whole body by using ultrahigh energy collimators with excellent resolution, which can minimize this problem [117- 118]. Their detection range reaches nano- to picomolar levels and is comparable to the one of the PET [119-120]. The resolution sensitivity is terms of 30 to 300 keV. They are cheaper and easier to handle than the one used for the PET, especially because of their longer half-live. The most utilized isotope is SPECT-scans remains ^{99m}Tc because of its convenient price and excellent radio-physical characteristics. SPECT systems are now widely used not only for human clinical purposes but also for early stage development of new drugs in small animals such as rats and mice. The radionuclides utilized for PET tracers have a very short half-life (2 minutes for ^{15}O , 20 minutes for ^{11}C and 10 minutes for ^{13}N), which makes the utilization of PET limited. A PET-scan requires a dedicated PET scanner, a specific cyclotron and a suitable chemical lab for the proper preparation of radiopharmaceuticals. SPECT is more advantageous when it comes to the preparation of the desired radionuclides, because its radionuclides have a longer half-life and are generally less challenging to synthesize. Commonly used γ -emitters for SPECT are ^{99m}Tc (Emax 141 keV, T1/2, 6.02 h), ^{123}I (Emax 529 keV, T1/2, 13.0 h) and ^{111}In (Emax 245 keV, T1/2, 67.2 h) [116]. SPECT imaging is much more widely available and less expensive than PET imaging. Furthermore, the resolution of microSPECT cameras (<0.5 mm) is even higher than that of the microPET ones (>1.5 mm) [116].

The strategy behind tumor imaging is to find a target that would ideally be present in all tumor stages and also would be possibly common to different types of cancer. Because cancer cells often change their features during growth stages, this has been challenging. It has been noticed that angiogenesis is a common characteristic to very many different types of cancer since the growth of all solid tumors is angiogenesis-dependent. Many receptors and factors play a role within this

complex process. Particularly viable are integrins receptors. Integrins have been detected in all types of tumors and are there essential for both, the tumor growth and the development of metastasis [66, 86]. Whenever it comes to targeting the integrin receptors, the ideal imaging method should allow to visualize and quantify integrin's expression before, during and after angiogenesis. Indirect and direct imaging methods have been developed. Direct imaging consists of labelling the target molecule itself, for example the integrin modulator VEGF, with a radioactive isotope such as ^{99m}Tc and then detecting it. A particular ^{99m}Tc radiolabeled VEGF compound was stable for 1 h and was detected in vivo for that amount of time on blood vessels [114]. The indirect method is based on labelling the receptor of the target molecule and not the molecule itself. In this case the most relevant example is the radiolabelling of RGD peptides to target the integrins as receptors.

The current trend in nuclear medicine is focused on combing different imaging techniques in order to be able to get more simultaneous information about the tumor's size, its structure and function. Combination of PET and CT can provide precise information about the tumor perfusion, its metabolism and its exact location, while PET together with MRI can increase the regular soft tissue contrast provided by MRI alone.

1.2. Integrins

1.2.1. Integrins in general

Integrins are part of a family of glycosylated, heterodimeric transmembrane adhesion receptors. They are responsible for cell–cell and cell–extracellular matrix (ECM) interactions, which include regulation of the adhesion to the ECM, organization and remodeling of the cytoskeleton, activation of intracellular signaling pathways, cell proliferation and control over the cell death or survival [29]. Integrins do not have any kinase activity, but they promote the activation of signaling pathways by clustering various proteins such as tyrosine kinases, focal adhesion kinase (FAK) and Src- family kinases [29, 32-33]. They are composed of one α and one β subunit. So far 8 β subunits and 18 α subunits have been discovered. Each different combination of the two subunits is unique and has specific binding and signaling characteristics [29]. Both subunits are glycoproteins and they are fixed in the cell membrane. The extracellular part is composed of the amino terminus and represents the main part of the peptide chain. The smaller part of the peptide, the C-terminus, is located in the inner part of the cell. This particular type of conformation allows these receptors to work in-and-out the cell membrane. The extracellular part of the alpha and beta chains works with a different mechanisms than the intracellular part. This enables both parts to transmit unique and differing signaling pathways to the inside or the outside of the cells. Whenever the ECM binds to the exterior part of the receptor, a signal is transmitted into the intracellular part. This makes it possible to convert extracellular ligand binding into activation of intracellular processes. Consequently, the activity of the integrins is regulated from the outside and the extracellular activity from the inside [29-30].

Based upon their ability of binding or not binding to ECM, integrin receptor determine the survival of physiological and/or tumor cells [31]. The ECM is a wide network of proteins secreted

by cells throughout their existence. There are two main types of ECM: the basal lamina and the interstitial matrix [29]. Both differ from each other in their structure and characteristics based on their location in the human body. Despite this, both have similar effects on the cells. They influence the migration, the proliferation and the apoptotic death of not only physiological cells but also cancerous ones [31]. It must be underlined that cells with neoplastic transformation are a lot less dependent on the extracellular matrix's adhesion than normal cells, but they still require integrins for processes like tumor initiation and tumor growth [105-106]. All these effects on the cells, promoted by the extracellular matrix, can only happen in the presence of activated integrins. In fact, activated integrins initiate signaling pathways that modify the cytoskeleton so that it can bind to the extracellular matrix. Aggregates composed of integrins, extracellular matrix proteins and the cytoskeletal proteins are then built on the inner and outer side of the membrane [29]. Integrins provide a sort of anchorage for the cells on the extracellular matrix that allows them to proliferate. Activating growth-promoting signaling influenced by ERK or MAPK contribute to this as well, but growth factors alone are not capable of initiating this pathway [39]. Cell proliferation could not occur if it was not for the integrins receptors.

Integrins are known to exist in various activation statuses with respectively different specificity and affinity for ligands. Integrins can often bind more than one ligand and a given ligand can attach to several integrins. The requirement for integrins to interact with different extracellular matrix components, is the presence on their surface of the correct amino acid sequence corresponding to their type. The Arg-Gly-Asp (RGD) sequence has been found on many matrix proteins including fibrinogen, vitronectin, fibronectin, thrombospondin, osteopontin, collagen and von Willebrand factor [83] and has been officially identified as a ligand for integrins such as $\alpha_v\beta_3$, $\alpha_v\beta_5$, and $\alpha_5\beta_1$ [40-43]. The presence of this sequence on so many relevant molecules

in the human body, makes it an excellent target to track various physiological and pathological processes. Macromolecular ligands containing the RGD sequence and capable of interacting with integrin $\alpha_v\beta_3$, have been synthesized to specifically target cancer related processes.

1.2.2. Integrins in cancer

Integrins play an essential role in the growth and development of a tumor. On a physiological basis they trigger many processes essential for normal cell functions and development. At the same time they are also directly responsible for pathophysiological mechanisms such as migration, proliferation and invasion that are basic requirements for the tumor growth [28]. In a cancerous environment, cells work differently than in a physiological one. In fact, tumor cells tend to lose those integrins that provide the attachment to the basement membrane. On the other hand integrins, which promote the tumor growth, are overexpressed during tumor angiogenesis. Integrins can be divided into two categories; the one promoting tumor growth and the other one preventing that. It has been found that integrin $\alpha_2\beta_1$ and $\alpha_3\beta_1$ correlate most frequently with tumor suppression, while integrin $\alpha_v\beta_3$, $\alpha_v\beta_6$ and $\alpha_6\beta_4$ are responsible for tumor promotion [31]. Integrins can so directly control the cell's lifecycles, by either sustaining cell survival or initiating apoptosis. So called ligated integrins promote survival signals, while unligated integrins stimulate pro-apoptotic cascades [72]. Ligated integrins promote cell survival through many mechanisms such as nuclear factor- κ B (nF- κ B) signaling [73] and/or p53 inactivation [74]. Unligated integrins are considered modulators of cell apoptosis [70]. They are involved in a process called integrin-mediated death (IMD), in which caspase 8 is recruited and activated by unligated integrins. The activation of the enzyme caspase 8 mediates the apoptotic cell death [75]. This particular mechanism is a key for the understanding of the tumor pathogenesis. Stupack et al. proved that the human cells can avoid IDM by losing caspase 8. They develop resistance to IDM which further supports tumor invasion

and metastasis [76].

In a cancerous environment, the cell cycle is mutated such that neoplastic cells can survive and grow even without the important requirements such as adhesion to the extracellular matrix [44-45]. They must undergo a complicated process made of several steps to spread out in the body. Tumor cells must first leave neighboring cells by destroying the basement membrane and going through the interstitial stroma [15]. In order for this to happen specific features of the extracellular must change. Under physiological a cell dissemination would never occur because anytime a cell would lose adhesion to ECM, it would physiologically die through apoptosis [31]. This process is called anoikis [71]. Surprisingly tumor cells do escape anoikis [54]. Once tumor cells have broken through the basement membrane, adherent junction between tumor cells must be separated to allow cells migration to the blood vessels [58]. Evidence shows that tumor cells must lose E-cadherin, an essential factor for cell-cell adhesion, in order to disrupt from adherent junctions [29]. This loss can either be genetically related or promoted by members of the SNAIL/SLUG family of transcription factors, which are able stop the transcription of the E-cadherin gene [92]. A process called intravasation begins when tumor cells switch to their migratory phenotype. Integrins are extremely important during tumor cell migration, because they influence gene expression and the cytoskeleton in way that it enhances this process. When migrating, tumor cells can enter either lymphatic or blood vessels. The invasion of blood vessels is more challenging, because it requires penetration of the basement membrane and destruction the cell-cell junctions. Lymphatic vessels are a lot easier to penetrate because they either a have basement membrane nor tight junctions [59]. Once tumor cells have reached a blood vessel, they must survive in the bloodstream. They accomplish this by attaching to platelets [60] or leukocytes [61-62], which protect them from the immune system and allow them to reach other organs. When tumor cells reach another organ, the

so called extravasation occurs and metastatic cells leave the bloodstream and grow further within the parenchyma of the target organ. Integrins strongly regulate several processes necessary for the invasion such as loss of cadherin-dependent junctions [47], loss of hemidesmosomes and acquisition of a motile invasive phenotype. The degradation of the basement membrane at the new tumor site is mainly caused by a protease called MMPs (matrix metalloproteinases). This protease remodels the extracellular matrix in a way that it makes it permeable to tumor cells [48]. MMPs are synthesized in an inactive status as pro-enzymes and are converted on site by autoproteolytic mechanism to their active form, which initiate matrix degradation [29, 51]. Integrin $\alpha_v\beta_3$ is directly responsible for recruiting and regulating MMP2 and plasmin.

The fact tumor cells do not die under usually rough conditions in many different foreign microenvironments is determined by different conditions [31]. This survival is mainly promoted by the loss of p53, FAK - a cell survival factor in many tumors - or by integrins themselves which stimulate the expression of BCL2, an anti-apoptotic factor and suppress the BCL2-family protein BIM, a pro-apoptotic factor [55-57]. Transforming Growth Factor- β related mutations are also commonly found in carcinomas. In a physiological environment this factor carries out a protective role because it prevents new forming neoplastic cells from proliferating by activating a cytostatic program that can stop their proliferation. In most types of carcinomas, a mutation makes them no longer responsive to TGF- β . In addition to this, in a terminal tumor stadium TGF- β can even interact with growth factors to further stimulate tumor growth and invasion [29].

1.2.3. Integrin $\alpha_v\beta_3$ in tumor angiogenesis

Integrin $\alpha_v\beta_3$ is expressed on the endothelial cells of most malignant tumors [66, 86], contributing to the growth of many types of cancer such as melanoma, ovarian, breast cancer and

glioblastoma [50, 67-68, 83, 87-88]. The expression of integrin $\alpha_v\beta_3$ is physiologically low on epithelial cells and mature endothelial cells, but it is higher on activated endothelial cells in the neovasculature of many tumors such as osteosarcomas, neuroblastomas, glioblastomas, melanomas and lung carcinomas [84-85]. The omnipresence of integrin $\alpha_v\beta_3$ on most types of cancers is the reason why it has the greatest potential to be a prognostic tumor indicator [86].

Integrin $\alpha_v\beta_3$, also called the vitronectin receptor, consists of two subunits: a 125-kDa α_v subunit and a 105-kDa β_3 subunit [82]. It interacts with many extracellular molecules such as fibronectin, fibrinogen, von Willebrand factor, vitronectin, proteolysed forms of collagen, laminin, fibroblast growth factor-2 (FGF2), metalloproteinase MMP-2, activated PDGF, insulin and the VEGF receptors [52-53, 13, 83]. The Arg-Gly-Asp (RGD) triple-peptide sequence is essential for the interaction between integrin $\alpha_v\beta_3$ and the previously listed extracellular molecules.

Integrin $\alpha_v\beta_3$ affects the tumor development more than any other integrin. It promotes its growth through several mechanisms that affect basement membrane destruction, adherent junctions separation, tumor migration and invasion [94, 14]. Interactions between integrins $\alpha_v\beta_3$ and RTKs as well as urokinase plasminogen activator receptor (uPA) sustain tumor cell migration [113,115]. Breakdown of the extracellular matrix is also promoted by integrin $\alpha_v\beta_3$ which recruits and activates MMP2 and plasminogen. MMP2 is a particular protease that can only be activated by binding to integrin $\alpha_v\beta_3$. Plasminogen must interact with integrin $\alpha_v\beta_3$ to be converted to plasmin and break down the extracellular matrix [10]. Interactions between integrin $\alpha_v\beta_3$ with specific growth factor receptors such as insulin-, platelet-derived growth factor- (PDGF), epidermal growth factor- (EGF) and vascular endothelial growth factor-receptor (VEGF) are also particularly important to sustain tumor proliferation [34-39]. Immune-precipitated $\alpha_v\beta_3$ integrin was found to be in a complex with the insulin-, the PDGF-, or the VEGF receptor [36]. The

aggregation of integrin $\alpha_v\beta_3$ with these growth factor receptors enables cross talk between them and is essential for their activation [37]. Particularly important is the interaction between integrin $\alpha_v\beta_3$ and VEGF. As a matter of fact, a study performed by Sarmishtha De et al. demonstrated that integrin $\alpha_v\beta_3$ is directly responsible for the expression of VEGF, which is initiated by the clustering of $\alpha_v\beta_3$ integrin [27]. The β_3 association with the phosphorylated p66 Shc is the prerequisite for the whole process to take place. A tumor must have an “activated” β_3 integrin in order to produce high levels of VEGF, required to sustain its blood vessel’s growth [27]. Integrin $\alpha_v\beta_3$ plays the role of a modulator between VEGF and its receptors within the process of angiogenesis [26].

Angiogenesis is the physiological process through which new blood vessels form from pre-existing vessels. The first formed cancerous spot is very small in size and is provided with nutrients and oxygen from pre-existing blood vessels surrounding the original tumor area. As soon as it grows beyond 2 mm in diameter, hypoxia starts to occur in the tumor, which together with inflammation and acidosis induces an overexpression of angiogenesis promoting factors. Whenever the pro-angiogenic factors become numerally more than the anti-angiogenic ones, a so called “angiogenic switch” occurs [1]. At this point the tumor “switches” to an accelerated angiogenic phenotype, allowing itself to grow increasingly faster [2, 11]. Folkman was the first one to carry out the idea a solid tumor starts out as a dormant not vascularized nodule that is only capable of expanding if it can build new blood vessels [3]. He hypothesized that the development of new blood vessels during angiogenesis derives from endothelial cells in pre-existing vessels. His hypothesis was recently rejected by demonstrating that tumor endothelial cells may also derive from circulating endothelial precursor cells originating in the bone marrow [4]. A recent study proved that bone marrow-derived cells are present in endothelial precursor cells in human cancer [5]. Triggers for neovascularization are many and include hypoxia, changes of the pH, metabolic

stress and cytokines from inflammatory response [6]. Certain oncogenes such as Src and Ras, androgen, progesterone and estrogen stimulate the process while tumor suppressor genes such as p53 down-regulate it [7-10].

1.2.4. Ligands for $\alpha_v\beta_3$

The omnipresence of integrin $\alpha_v\beta_3$ in so many types of tumors makes it a useful target for diagnosis and therapy purposes. Studies using $\alpha_v\beta_3$ antagonists such as monoclonal antibodies (mAbs), cyclic RGD peptide antagonists and peptidomimetics demonstrated that blocking $\alpha_v\beta_3$ induces endothelial cell apoptosis and can prevent further angiogenesis from occurring [86, 89]. These so called anti-angiogenic agents aim to block the development of new blood vessels. As a consequence of this, the tumor will “starve” because it does not get enough oxygen and supplements from the blood. Decrease in the activity of integrin $\alpha_v\beta_3$ correlates with lower tumor growth in breast cancer xenografts [90-91]. This proves that by antagonizing integrin $\alpha_v\beta_3$, inhibition of the tumor growth occurs [83].

Among all the synthesized integrin $\alpha_v\beta_3$ antagonists, peptides have become more popular for imaging purposes for their several advantages. Their favorable size allows good tumor targeting and penetration [121]. Their small proportion (MW < 10.000 Da) gives them the advantage of reaching the tumor cells faster than any other type of antibody. At the same time a fast clearance due to the small size ensures a fast elimination. This keeps the contact time with human body short, so minimizing the potential adverse effects. Another advantage in the use of peptides is their easy synthesis that can simply occur with the help of a conventional peptide synthesizers.

1.3. Radiopharmaceuticals

Radiopharmaceuticals are so called because they consist of two components: a pharmaceutical and a radioactive one. These compounds find usually application in nuclear medicine as intravenous drugs for the therapy and the diagnosis of different diseases. Because they are administered to humans, they are required - as any other intravenous drug - to be sterile and pyrogen-free. Furthermore they must meet the basic quality control requirements of any drug.

Based upon how they are utilized, radiopharmaceuticals can be categorized as diagnostic or therapeutic radiopharmaceuticals. Diagnostic radiopharmaceuticals are radiolabelled with gamma-emitting isotopes and can be used for both SPECT and PET. They are injected in low doses that do not cause a pharmacological effect on the body [77]. They are called diagnostic radiopharmaceuticals because they contribute to the detection of diseases. If the disease has been already diagnosed, they can provide information about its status and development. The uptake of the radiotracer in a certain organ or tissue provides helpful information about its morphologic structure and physiological function. Part of this category are the ^{111}In - radiolabeled cyclic RGD dimers used in our experiments. The second group of radiopharmaceuticals is constituted of therapeutic radiotracers, which carry higher activities of specific radionuclides. Their purpose is to reach the desired localization and to deliver there the cytotoxic radiation dose. In order to harm other organs with the least possible amount of radiation, they should have a fast clearance.

There are important parameters that must be considered when developing a radiopharmaceutical. Its physicochemical characteristics should be similar to the one of the non-radiolabeled molecule they are linked. The effective half-life, which is influenced by either biological elimination or the natural physical decay of the radionuclide, should be as short as possible to avoid excessive radioactive exposure for the patient. At the same time it should to be

long enough to enable the study or the therapy session to take place. Another characteristic that ideal radiopharmaceutical should have is a wide, diagnostically useful target-to-non-target activity, also called target-to-background (T/B). This is essential to ensure a not too high uptake of the tracer in non-target areas because this could potentially weaken the contrast towards the desired areas. The non-target-radioactivity can be decreased by fast blood clearance of the tracer. On the other hand, the target-radioactivity can be increased by either making sure that the radioactive agent will get to the target as fast as possible or by assuring that its binding rate is fast and its dissociation rate slow [83]. The stoichiometry and charge of the radioactive agent are also important physicochemical characteristic of a radiopharmaceutical. The charge has a relevant impact on the solubility of the radioactive molecule. A partial solubility in water is essential for the injection of the radiopharmaceutical into the human or animal body. Furthermore, the pH of the injected solution must be compatible with the one of the blood (7.4). The lipophilic grade of the compound determinates where the radioactive compound will be accumulated. The availability, plasma clearance, tissue distribution and most importantly the uptake in the desired organ are affected by the grade of protein binding to the radiopharmaceutical in the plasma. Transferrin is the plasma-protein that binds many metallic radionuclides found in radiopharmaceuticals. Metal chelates in radiopharmaceutical tend to donate their ions to transferrin in plasma because metals have a very high affinity to this protein. This can have negative consequences for the stability of the radioactive agent, because in vivo breakdown of the complex can occur leading to biodistribution of radioactivity. Physicochemical stability of a radiolabeled molecule is one of the most difficult issues to accomplish, because it is affected by many variables such as temperature, pH, light and protein binding. Within the development of a new radiopharmaceutical the most valuable test to verify its efficacy and its stability is the biodistribution study. Such a study includes

the measurement of the radioactivity in the different organs as well as tissue distribution, plasma clearance, urinary and fecal excretion after intravenous injection of the radiopharmaceutical. An important pharmacokinetic parameter that must be considered for receptor targeting agents is the receptor binding rate, which should be as fast as possible to achieve the highest accumulation at the target site. The clearance of the compound from the kidneys should be rapid to minimize an unwanted uptake of the radioactive agent in the gastrointestinal tract.

The development of a radiopharmaceutical starts out with the identification of the target biomolecule that will carry the radioisotope to the target organ or tissue. Second, a radionuclide with possibly small influence on the biochemical and pharmacological characteristics of the original non-radiolabeled-biotarget must be found. It is important to remember that the radiolabelling is the most challenging step of the radiosynthesis. In fact, if not done correctly, it could have a negative influence on the binding affinity to the receptor. Finding the right labeling position, as far away as possible from the binding site, is essential to avoid this problem [78]. It is essential to find out if the radionuclide can be incorporated into the chosen molecule or not, because this strongly correlates with the type of radiolabelling to choose.

Once the appropriate radionuclide and target biomolecule are found, a preparation procedure needs to be developed based upon the physicochemical characteristics of the compound. This includes a protocol containing all the necessary information about the synthesis of ligand, the radiolabelling and the stability of the radioactive compound. The preparation should be possibly simple and easy to reproduce and it should ensure that ideal physicochemical conditions such as temperature, pH, ionic strength and molar ratios stay unvaried throughout and after the preparation, in order to guarantee the maximal efficacy of the radiopharmaceutical. Once a successful strategy is developed, the radioactive compound must first undergo an evaluation in animals. If the toxicity

does not interfere, a clinical evaluation takes place in humans to test the efficacy of the radiopharmaceutical.

1.3.1. Radiolabeled peptides and their development

A radiolabelled peptide is composed of three main components: the targeting biomolecule (BM), the pharmacokinetic modifying linker and radioactive chelate (Figure 2).

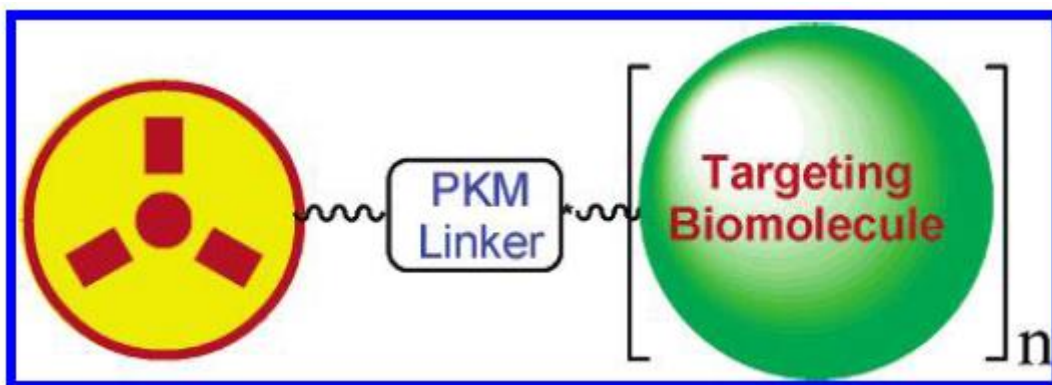


Figure 2 - The three components of a radiopharmaceutical (Radiolabeled Multimeric Cyclic RGD Peptides as Integrin $\alpha_v\beta_3$ Targeted Radiotracers for Tumor Imaging, Shuang Liu, 2006, Molecular Pharmaceutics, Vol.3 N. 4, pp. 474)

In the case of integrin $\alpha_v\beta_3$ radiotracer, the targeting biomolecule is the cyclic RGD peptide. Its purpose is to lead the radionuclide to the integrin $\alpha_v\beta_3$ on the tumor cells [83]. The targeting molecule must be identified as first, with either autoradiography or immunohistochemistry. Second, receptor density needs to be considered in order to obtain a successful targeting. The desired peptide can then be synthesized based upon the chemical structure of the physiological ligand. Finally, the radioactive isotope is attached to the compound. A peptide is mostly labeled through an indirect labeling method, which only requires an already established radiotracer to be bond to the targeting biomolecule. This method is widely used to label bigger molecules such as peptides and antibodies. Most peptides used for nuclear medicine purposes are labeled with an indirect

method, because the larger the molecule, the less influence will the isotope have on its biocharacteristics.

A commonly used isotope in gamma scintigraphy or single photon emission computed tomography (SPECT) is the hard lewis acid In^{3+} . It has a high charge density and a small ionic radius. It can form high stability complexes with hard ligands containing nitrogen and oxygen as donor atoms [160]. ^{111}In has two gamma emissions with the photon energy of relatively 173 and 247 keV. The first ^{111}In labeled peptide for clinical purposes was DTPA-octreotide (diethylenetriaminepentaacetic acid), which was utilized to detect neuroendocrine tumors [92]. Cyclic RGD peptides have also been labeled with ^{111}In , proving that it fulfills all the requirements an isotope should have for tumor imaging purposes [63, 64]. There are three relevant radiolabelling approaches for peptides: the integrated, the bifunctional and the hybrid radiolabelling (Figure 3) [77]. The integrated approach requires part of the receptor-binding-ligand to be replaced with a metal chelate. Once metal chelation occurred, the whole molecule becomes the new high affinity receptor ligand. In the bifunctional approach, the procedure is different. Therefore the radiopharmaceutical required components are combined together: the high affinity receptor ligand as the targeting biomolecule, a BFC for conjugation of the receptor ligand, a radiometal for the chelation and a linker for possible pharmacokinetic modification. This approach is the most commonly used. The majority of the RGD peptides were radiolabeled with this method. It must be ensured that the radiopharmaceutical is built in a way that the radiometal chelate is not close to the receptor binding part of the compound. This will avoid any undesired interaction with the receptor that could potentially compromise the binding affinity [77]. The chelation of the radiometal is an crucial step in the development of a radiolabeled peptide, because it can increase the binding affinity of the peptide sequence. Macrocyclic chelators have taken over

the acyclic ones because of their favorable thermodynamical stability. Their excellent pharmacokinetics have contributed to the wide utilize of the cyclic polyaminopolycarboxylic ligands such as DOTA and NOTA, particularly in combination with trivalent metals such as In^{3+} [93-96].

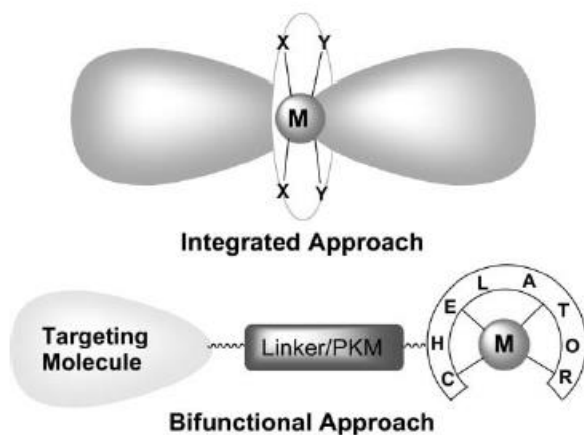


Figure 3 - Radiopharmaceutical design (The role of coordination chemistry in the development of target- specific radiopharmaceuticals, Shuang Liu, Chem. Soc. Review, 2004, 33, p. 447)

DOTA is capable of binding radioactive metal ions in strong coordination complexes of up to eight dative bonds. This BCA was synthesized for the first time in 1967 by Stetter and Frank [106]. The excellent kinetic stability of complexes with DOTA makes it the most widely used chelator for radiopharmaceutical use. This is why clinical use of DOTA-peptide conjugates labeled with ^{68}Ga and ^{111}In is nowadays as widely spread as somatostatin conjugates such as DOTA-TOC and DOTA-TATE [107, 98]. NOTA has a smaller ring structure in comparison to DOTA and only has 3 chelating carboxylate groups and 3 nitrogens. It has 6 coordination sites with metal ions. The difference between NOTA and DOTA is based on the differing cavity size, which has a big influence on the thermodynamic stability of the compounds, making $^{67/68}\text{Ga}$ -NOTA complexes about 10 orders higher than that of $^{67/68}\text{Ga}$ -DOTA [81]. NOTA's downside is its complicated

coupling process to the peptides, which has only been described in few papers. The easiest way to attach NOTA is through a multiple step de novo synthesis on solid support [69, 77]. During such a synthesis, a coupling moiety is introduced at the α -position of a carboxylate arm such as aspartic acid (NODASA), glutamic acid (NODAGA) or benzyl-isothiocyanate (NODAPA-NCS).

No matter what radiolabelling approach is chosen, the ideal labeling procedure should ensure a high labelling yield and radiochemical purity. Once the radio-synthesis protocol is optimized, in vitro evaluation takes place. Binding studies using cells or cell membrane must provide evidence of a high binding affinity to the tumor cells, while the affinity to non-target tissue such as the gastrointestinal tract should be as low as possible. In fact, a high tracer uptake in the wrong organ could be easily misunderstood for a misplaced tumor activity. Peptides are additionally required to be amenable to chemical/molecular modifications and their ability to attach a chelating agent at the C- or N-terminus of the peptide is essential. Unfavorable pharmacokinetic characteristics can be modified with molecular engineering techniques, for example by altering the peptide sequence during the synthesis or by adding a bio-modifying molecule [122]. The addition of linkers to combine molecules, the use of spacers to modify the distance or the modification of the amino acid sequence are simple but widely applied strategies to improve peptide's chemical and pharmacokinetic properties. Biological interactions of the radiopharmaceutical also need to be evaluated in order to avoid unwanted interactions with the radioactive agent in vivo, which could lead to radiation toxicity.

1.3.2. Radiolabeled peptides for integrins $\alpha_v\beta_3$

The use of peptides to track angiogenesis has become popular since Haubner et al. had created the first radiolabeled RGD peptide markers to target integrin $\alpha_v\beta_3$. Their tumor affinity,

particularly the one for melanoma M21 cells was promising [124]. Furthermore, the blockade of integrin $\alpha_v\beta_3$ led to apoptosis of activated endothelial cells expressing them [125]. After this discovery, it was proven that peptides containing the amino acid sequence Arg-Gly-Asp are specific antagonists for integrin $\alpha_v\beta_3$. Histological tests confirmed this, by providing evidence of the presence of an interaction between RGD and integrin $\alpha_v\beta_3$ on tumor cells [122]. RGD tracers became so a new way to target microvascular density in tumors because, by binding to integrin $\alpha_v\beta_3$ on endothelial cells of new forming blood vessels, they can track angiogenesis [126]. More studies demonstrated that through the antagonism to integrin $\alpha_v\beta_3$, RDG peptides are able to inhibit angiogenesis and stimulate regression of the tumor by slowing down its growth throughout blood vessels [78, 80, 109]. In order for this to happen, IC50 values should be in the nanomolar range and the RDG peptide should show a higher selectivity for integrin $\alpha_v\beta_3$ over glycoprotein IIb/IIIa (GPIIb/IIIa) [77]. Since Haubner created the first radiolabeled RGD peptide, many others have been synthesized for both PET and SPECT imaging purposes [127]. The first clinical tests with RGD tracers in a clinical environment had good results with a tumor to background activity similar to the one of FDG-PET [128]. The main concern was the fast excretion from the body due to a fast kidney's and/or liver's clearance [129]. In order to avoid this, the affinity between RGD peptide tracer and the integrin receptors needed to be increased. Several modifications of the original structure have been carried out in order to optimize the chemical characteristics and the pharmacokinetics of the compounds. Cyclic RGD peptides with a significant better integrin selectivity and a higher chemical stability than the original linear ones were created. Linkers such as S-S disulfides, thioethers, aromatic rings or heterocycles have been used to achieve cyclisation [77]. Based on the IC50 value, Aumailley et al. were able to prove that the cyclic pentapeptide “cyclo(Arg-Gly-Asp-D-Phe-Val)” is a 100 times better inhibitor of cell adhesion to the vitronectin

than the linear version of the peptide [97]. Several studies have provided evidence that cyclic peptides have better pharmacological and pharmacokinetic characteristics such as higher binding affinity and increased selectivity for integrin $\alpha_v\beta_3$ [29]. Other chemical modifications of cyclic peptides have been evaluated and reviewed [83]. It was proven that the amino acid in position 5 has no significant impact on the integrin $\alpha_v\beta_3$ binding affinity. Another amino acid in the RGD peptide sequence gathered particular attention: It was the valine (V) in the cyclic RGD peptide c(RGDfV). This amino acid can be potentially replaced by lysine (K) or glutamic acid (E), generating new compounds, respectively c(RGDfK) and c(RGDfE), with no impact on the integrin $\alpha_v\beta_3$ binding affinity but rather improved the pharmacokinetics [83]. The addition of a hydrophobic amino acid in position 4 also seemed helpful in increasing the binding affinity to integrin $\alpha_v\beta_3$ [29]. Another attempted modification was the conjugation of RGD peptides with sugar amino acids. These new compounds, called glycopeptides, showed favorable characteristics such as increased accumulation in the liver, higher blood levels, uptake and retention in the tumor when compared to the regular peptides [63]. Decristoforo et al. demonstrated that ^{99m}Tc -labeled RGD peptides derivatized with HYNIC (^{99m}Tc -HYNIC-RGD) can be excellent tools to gather integrin $\alpha_v\beta_3$ related images [16, 17, 20]. Other modifications were attempted, in order to improve the chemical and pharmaceutical characteristics of RGD peptides, but cyclization remained the best improvement that was accomplished, until multimerisation was introduced. So called multimeric RGD peptides composed of more than one peptide such as dimers, tetramers and octamers became better targeting biomolecules for integrin $\alpha_v\beta_3$ radiotracers (Figure 4). The first ^{99m}Tc labeled dimers - E[c(RGDfK)]₂ - were developed by Rajopadhye et al. for diagnostic purposes [108]. Poethko et al. carried out the hypothesis that dimers have even higher binding affinity to integrin $\alpha_v\beta_3$ and better tumor uptake than monomers. This was demonstrated with the

RGDfE dimer [c(RGDfE)HEG]₂- K-Dpr-[¹⁸F]FBOA [152, 99]. A group of cyclic RGDfK tetramers were prepared by Boturn et al., who stated that there is a correlation between peptide multiplicity and a significantly higher integrin $\alpha_v\beta_3$ binding affinity and internalization [100]. Another cyclic RGDfK tetramer E[E-[c(RGDfK)]₂]₂ was discovered by Liu et al. as a targeting biomolecule for SPECT and PET radiotracers detecting integrin $\alpha_v\beta_3$ [101]. The main idea behind multimeric peptides is that a local higher RGD concentration correlates with higher tumor uptake. Radiolabeled cyclic RGD dimers accumulate more in the tumor than their monomeric analogues [8, 9, 12, 102]. Moreover, it was demonstrated that tetramers and octamers have a higher tumor uptake and integrin affinity than their analogs dimers. Multimerisation is a key to improve the affinity to integrin $\alpha_v\beta_3$. However, multimeric peptides have a higher accumulation in non-target organs such as liver, lungs and kidneys [104]. The concept of bivalency made it possible to minimize this problem. Bivalency is based on the distance between two cyclic RGD modifications. The ability of a multimeric cyclic RGD peptide to develop bivalency is greatly influenced by the integrin $\alpha_v\beta_3$ density on tumor cells and tumor neo-vasculature. If the density is high, the distance between two neighboring integrin sites will be short. Short distance is a favorable factor for a multimeric RGD peptide to develop bivalency. On the contrary, if two integrin sites are far part - for example because of low density due to tumor's tissue necrosis - it will be difficult for the peptide to bind to two different integrin sites at the same time. In this case the two RGD peptides of one compound would need to be further apart in order to bind at the same time to more than one integrin $\alpha_v\beta_3$. This is more difficult to establish when using a single multimeric peptide [83]. The bivalency factor carries out its biggest potential in multimeric compounds. Liu et al. explained that a dimer with only two cyclic modification has just a single possibility to gather the bivalency. A tetramer with four RGD modifications is more likely to establish bivalency because any two of

those four modification can be used, based on the distance between the integrin sites. It is important to underline that not all multimeric peptides can be multivalent. The binding affinity of peptides that can not establish bivalency, can be improved by the so called concentration factor”.

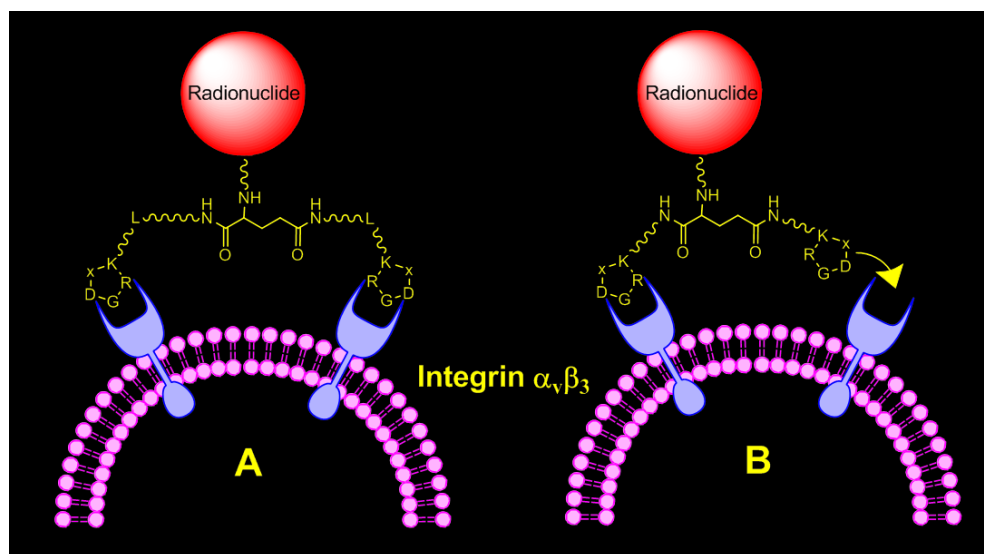


Figure 4 – Interaction between cyclic RGD peptide dimers and integrin $\alpha_v\beta_3$ (Radiolabeled Cyclic RGD Peptides as Integrin $\alpha_v\beta_3$ -Targeted Radiotracers: Maximizing Binding Affinity via Bivalency, Shuang Liu, Review, Bioconjugate Chemistry, 2009, Vol. 20, Number 12, pp. 2205)

The idea behind this, is that a higher local RGD concentration correlates with a greater tumor uptake [102]. Bivalency is hardly found in dimers because the space between the two modifications is too short. However, the so called “locally enriched concentration” established by a dimer, can improve its binding affinity [103]. The local concentration at the integrin $\alpha_v\beta_3$ site is increased by the presence of second RGD motif. As a consequence, the binding affinity of the dimer to that receptor will be higher compared to its analog monomer. An example for this is the dimer DOTA-P-RGD2, which has the better integrin $\alpha_v\beta_3$ binding affinity than its equivalent monomer DOTA-P-RGD [104].

To conclude, both bivalency and the “locally enriched RGD concentration” provided by multimerisation are essential to increase the $\alpha_v\beta_3$ binding affinity of RGD peptides.

2. Evaluation of ^{111}In -Labeled Dimeric Cyclic RGD :

^{111}In (DOTA-Galacto-RGD₂) and ^{111}In (NOTA-Bz-Galacto-RGD₂)

Project Aims.

The topic I focused my attention on are radiolabeled cyclic RGD peptide dimers as PET or SPECT radiotracers for molecular imaging of solid tumors. The aim of this thesis project was the evaluation of ^{111}In (DOTA-Galacto-RGD₂) (Figure 7: DOTA = 1,4,7,10-tetraazacyclododecane-1,4,7,10-tetracetic acid) and ^{111}In (NOTA-Bz-Galacto-RGD₂) (Figure 7: 1,4,7-triazacyclononane-N,N',N''-triacetic acid) (NOTA-Bz = 2-(p-thioureidobenzyl)-1,4,7-triazacyclononane-1,4,7-triacetic acid) as new integrin $\alpha_v\beta_3$ -targeted SPECT radiotracers for breast tumor imaging. We wanted to compare DOTA, which has been widely used as the bifunctional chelator for ^{64}Cu , ^{68}Ga , ^{90}Y , ^{177}Lu and ^{111}In -labeling of peptides and small biomolecules and NOTA, another bifunctional chelator for ^{64}Cu and ^{68}Cu , that has the advantage of having an extremely high solution stability [143, 144, 145-157]. With this study we aimed to compare and evaluate the tumor uptake and biodistribution of ^{111}In (DOTA-Galacto-RGD₂), ^{111}In (NOTA-Bz-Galacto-RGD₂) and ^{111}In (DOTA-3P-RGD₂) in the same tumor-bearing animal model.

Whatmore, we wanted to find out what impact the combination of SAA, PEG₂ and 1,2,3-triazole groups had on ^{111}In -Galacto-RGD₂, after positive reviews regarding a reduced radioactivity accumulation for in normal organs, such as intestines, lungs and spleen for $^{99\text{m}}\text{Tc}$ -Galacto-RGD₂ [142].

Materials and Experimental Procedure

Materials and Instruments.

All chemical and solvents were purchased from Sigma/Aldrich (St. Louis, MO) and used without further purification. Biodistribution and planar imaging studies were done using the athymic nude mice bearing MDA-MB-435 breast tumor xenografts. This animal model has been already widely used previously showing good evidence at evaluating radiolabeled cyclic RGD peptides as radiotracers [158-160]. We used MDA-MB-435 breast tumor cell line despite the controversy related to its identity [161-163]. More recent results provided evidence for that fact that MDA-MB-435 is a not highly differentiated but aggressive breast tumor cell line [165].

Synthesis of Galacto-RGD₂ peptides

The synthesis of the galacto-RGD₂ peptides, their physicochemical characteristics, their purification and HPLC methods took place at Purdue in Dr. Liu Shuang's lab prior to my arrival and are accurately explained in the annex. I did not take part of the experiments regarding the radiochemical synthesis.

HPLC Method for ¹¹¹In-labeled RGD Dimers.

The radio-HPLC used the LabAlliance HPLC system equipped with a β -ram IN/US detector (Tampa, FL) and Zorbax C₁₈ column (4.6 mm x 250 mm, 300 Å pore size; Agilent Technologies, Santa Clara, CA). The flow rate was 1 mL/min. The mobile phase was isocratic for the first 5 min with 90% A (25 mM NH₄OAc, pH = 6.8) and 10% B (acetonitrile), followed

by a gradient mobile phase going from 90% A and 10% B at 5 min to 60% A and 40% B at 20 min.

Tumor Cell Culture.

The U87MG and MDA-MB-435 cell line were obtained from ATCC (American Type Culture Collection, Manassas, VA). Tumor cells were cultured in the Minimum Essential Medium, Eagle with Earle's Balanced Salt Solution (non-essential amino acids sodium pyruvate), and were supplemented with 10% fetal bovine serum (FBS, ATCC) and 1% penicillin and streptomycin solution (GIBCO Industries Inc., Langley, OK) at 37 °C in a humidified atmosphere of 5% CO₂ in air. Cells were grown as monolayers and were harvested or split when they reached 90% confluence to maintain exponential growth. ¹¹¹InCl₃ was obtained from Perkin-Elmer Life Sciences (North Billerica, MA). The NH₄OAc buffer for ¹¹¹In-labeling was passed over a Chelex-100 column (1x15 cm) to minimize the trace metal contaminants. To a 2 mL clean Eppendorf tube were added 200 μL of the solution containing DOTA-Galacto-RGD₂ or NOTA-Bz-Galacto-RGD₂ (2.5 mg/mL in 0.1 M NaOAc buffer, pH = 5.0 – 5.5) and 50 – 100 μL of ¹¹¹InCl₃ solution (0.5 – 1.0 mCi in 0.05 M HCl). The tube was sealed, and then heated in a boiling water bath for 15 min. A sample of the resulting solution was analyzed by radio-HPLC (Method 2).

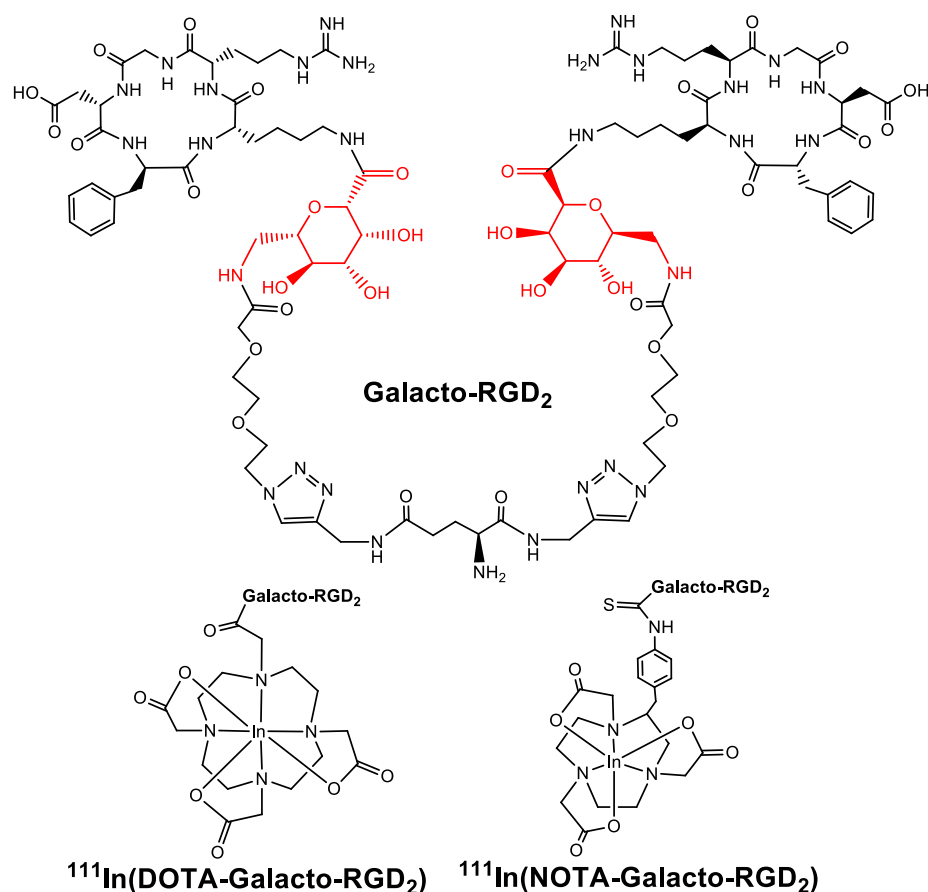


Figure 7. Structure of Galacto-RGD₂ and its ¹¹¹In complexes: ¹¹¹In(DOTA-Galacto-RGD₂) and ¹¹¹In(NOTA-Galacto-RGD₂). The 7-amino-L-glyero-L-galacto-2,6-anhydro-7-deoxyheptanamide (SAA) and 1,2,3-triazole moieties are used to minimize its accumulation in healthy organs, such as intestines, liver, lungs and spleen.

¹¹¹In-Labeling and Dose Preparation.

Doses for biodistribution were made by dissolving the ¹¹¹In radiotracer in saline to ~30 μCi/mL. For blocking experiment, excess RGD₂ was dissolved in the dose solution to 7.5 mg/mL. For planar imaging, doses were prepared by dissolving radiotracer in saline to ~1 mCi/mL. In all cases, the dose solution was filtered with a 0.20 μm Millex-LG filter before being injected into animals. Each animal was administered with ~0.1 mL of the dose solution.

In Vitro Whole-Cell Integrin $\alpha_v\beta_3$ Binding Assay.

Integrin $\alpha_v\beta_3$ binding affinity of DOTA-Galacto-RGD₂ and NOTA-Bz-Galacto-RGD₂ was determined in a whole-cell displacement assay and compared to that of DOTA-3P-RGD₂ (3P-RGD₂ = PEG₂-E[PEG₄-c(RGDfK)]₂; and PEG₄ = 15-amino-4,7,10,13-tetraoxapentadecanoic acid). ¹²⁵I-echistatin (Perkin Elmer, Branford, CT) as the integrin-specific radio-ligand [2, 3, 9] for the cellular competitive displacement assay. The U87MG cell line was obtained from ATCC (American Type Culture Collection, Manassas, VA). Filter multiscreen DV plates (Millipore, Billerica, MA) were seeded with 1×10⁵ U87MG human glioma cells in the binding buffer (20 mM Tris, 150 mM NaCl, 2 mM CaCl₂, 1 mM MnCl₂, 1 mM MgCl₂, 0.1% (wt/vol) bovine serum albumin (BSA); and pH 7.4) and ¹²⁵I-echistatin (0.75 – 1.0 kBq) in the presence of increasing concentrations of cyclic RGD peptide conjugates, incubated for 2 h at room temperature. After removing unbound ¹²⁵I-echistatin, the hydrophilic PVDF filters were washed 3x with the binding buffer, and then collected. Radioactivity was determined using a Perkin Elmer Wizard – 1480 γ - counter (Shelton, CT). Experiments were carried out twice with triplicates. IC₅₀ values were calculated by nonlinear curve fitting experimental data using GraphPad Prism™ (GraphPad Prism 5.0, San Diego, CA) and were reported as an average plus/minus standard deviation.

NOTA-Galacto-RGD ₂	$Y = 16.44 + 81.61/(1+10^{X+7.623})$
DOTA-Galacto-RGD ₂	$Y = 25.39 + 65.06/(1+10^{X+7.573})$
DOTA-3P-RGD ₂	$Y = 26.89 + 65.21/(1+10^{X+7.541})$
DOTA-3P-RGK ₂	$Y = 22.49 + 68.69/(1+10^{X+6.224})$
c(RGDfK)	$Y = 17.45 + 79.56/(1+10^{X+6.383})$

Animal Model.

Biodistribution and imaging studies were performed using the athymic nude mice bearing U87MG human glioma xenografts in compliance with NIH animal experiment guidelines (Principles of Laboratory Animal Care, NIH Publication No. 86-23, revised 1985). The animal

protocol has been approved by the Purdue University Animal Care and Use Committee. Female athymic nu/nu mice were purchased from Harlan (Indianapolis, IN) at 4 – 5 weeks of age. Each mouse was implanted subcutaneously with 5×10^6 MDA-MB-435 cells into the fat pad. Four weeks after inoculation, tumor size was 0.1 – 0.4 g, and animals were used for biodistribution and imaging studies.

Biodistribution Protocol.

Sixteen to twenty tumor-bearing mice (20 – 25 g) were randomly divided into five groups into the 1h group, the 4h group, the 24h group, the 72h group and the RGD blocking group. Each tumor-bearing mouse was administered with $\sim 3 \mu\text{Ci}$ of the ^{111}In radiotracer by tail vein injection. The injected dose for each mouse was calculated by mean counts per gram considering the weight difference of each syringe (injected for mice) before and after 0.1 mL ^{111}In -NOTA-Bz-Galacto-RGD₂ was injected. Animals (4 – 5) were sacrificed by sodium pentobarbital overdose (~ 200 mg/kg) at 1, 4, 24 and 72 h post-injection (p.i.). Blood samples were withdrawn from the heart of tumor-bearing mice. The tumor and normal organs (brain, eyes, heart, spleen, lungs, liver, kidneys, muscle and intestine) were harvested, washed with saline, dried with absorbent tissue, weighed, and counted on a Perkin Elmer Wizard – 1480 γ -counter (Shelton, CT). The organ uptake was calculated as the percentage of injected dose per gram of organ mass (%ID/g) or the percentage of injected dose per organ (%ID/organ). After the injection, the radioactivity in the syringe and on the gauze were measured and subtracted from the total radioactivity injected previously in order to have the most precise and accurate results.

For the blocking experiment, five tumor-bearing athymic nude mice (20 – 25 g) were used, and each animal was administered with $\sim 3 \mu\text{Ci}$ of ^{111}In (DOTA-6P-RGD₄) along with $\sim 350 \mu\text{g}$ (~ 14

mg/kg) of RGD₂. Such a high dose of RGD₂ was used to make sure that the $\alpha_v\beta_3$ integrin binding was completely blocked. At 1 h p.i., all five tumor-bearing animals were sacrificed for organ biodistribution. Biodistribution data (%ID/g) and target-to-background (T/B) ratios are reported as an average plus/minus standard deviation based on the results from 4 – 5 tumor-bearing mice at each time point. Comparison between two radiotracers was made using the one-way ANOVA test (GraphPad Prim 5.0, San Diego, CA). The level of significance was set at $p < 0.05$.

Planar Imaging.

Animals bearing MDA-MB-435 breast cancer xenografts were used for planar imaging with ¹¹¹In(DOTA-Galacto-RGD₂) and ¹¹¹In(DOTA-3P-RGD₂). Tumor-bearing mice were anesthetized with intraperitoneal injection of Ketamine (40 – 100 mg/kg) and Xylazine (2 – 5 mg/kg). Each animal was administered with ~100 μ Ci of ¹¹¹In radiotracer. Animals were placed on a single head gamma camera (Diagnostic Services Inc., NJ) equipped with a parallel-hole, medium-energy, and high-resolution collimator. Static images were acquired at 1, 4 and 24 h p.i. and stored digitally in a 128 x 128 matrix. The acquisition count limits were set at 500 K. For the blocking experiment with ¹¹¹In(DOTA-Galacto-RGD₂), RGD₂ (~14 mg/kg or ~350 μ g per 25 g tumor-bearing mouse) was co-injected as the blocking agent. After planar imaging, animals were euthanized by sodium pentobarbital overdose (100 – 200 mg/kg).

Tumor Tissue Immunohistochemistry.

Tumors were harvested, were snap-frozen in the OCT (optical cutting temperature) solution (Sakara, Torrance, CA), and cut into slices (5 μ m). After drying at room temperature, the slides were fixed with ice-cold acetone, and dried in the air for 20 min at room temperature. The sections

were blocked with 10% goat serum for 30 min at room temperature, and then were incubated with the hamster anti-integrin β_3 antibody (1:100, BD Biosciences, San Jose, CA) and rat anti-CD31 antibody (1:100, BD Biosciences) for 1 h at room temperature. After incubating with the Cy3-conjugated goat anti-hamster and FITC-conjugated (fluorescein isothiocyanate) goat anti-rat secondary antibodies (1:100, Jackson ImmunoResearch Inc., West Grove, PA) and washing with PBS buffer, the fluorescence was visualized with a Nikon microscope. All pictures were taken under 200x magnification with the same exposure time. The specificity of the antibody was assessed by incubating the negative control only with the secondary antibody.

Cellular Immunostaining.

MDA-MB-435 human breast cells were seeded into 8-well chamber slides (BD Biosciences, Franklin Lakes, NJ), and were allowed to attach and spread for >24 h. Tumor cells were then fixed in -20 °C methanol for 5 min and rinsed with PBS. Cells were incubated in 5% BSA for 30 min to block nonspecific binding, and then incubated with rabbit anti-human and murine integrin β_3 antibody followed by incubation with Alexa Fluor 594 conjugated goat anti-rabbit IgG (Santa Cruz, CA). After washing with PBS, the slides were mounted with Dapi-Fluoromount-G (SouthernBiotech, Birmingham, AL). The fluorescence was visualized with a Nikon fluorescence microscope (Nikon Instruments, Melville, NY). The same experiment was repeated three times independently. By incubating the negative control only with the secondary antibody, the specificity of the antibody was assessed.

3. Results

Radiochemistry.

$^{111}\text{In}(\text{DOTA-Galacto-RGD}_2)$ and $^{111}\text{In}(\text{NOTA-Galacto-RGD}_2)$ were prepared from the reaction of $^{111}\text{InCl}_3$ with DOTA-Galacto-RGD₂ and NOTA-Galacto-RGD₂, respectively, in NH₄OAc buffer (100 mM, pH = 5.5). Radiolabeling was completed by heating the reaction mixture at 100 °C for ~15 min. Radiochemical purity was >95% with a specific activity of > 40 mCi/μmol. $^{111}\text{In}(\text{DOTA-Galacto-RGD}_2)$ and $^{111}\text{In}(\text{NOTA-Galacto-RGD}_2)$ remained stable for more than 72 h in the kit reaction matrix or in the presence of 5 mM EDTA.

Integrin $\alpha_v\beta_3$ Binding Affinity.

Figure 5 shows displacement curves of ^{125}I -echistatin bound to U87MG glioma cells in the presence of cyclic RGD peptide conjugates. The IC₅₀ values were calculated to be 24±4, 27±2, 29±4, 596±48 and 414±36 nM for NOTA-Galacto-RGD₂, DOTA-Galacto-RGD₂, DOTA-3P-RGD₂, DOTA-Galacto-RGK₂ and c(RGDfK), respectively. We so performed a total of 5 experiments by using c(RGDfK) as standard for the in vitro displacement assay. 3P-RGK₂ was the non-sense peptide to demonstrate the RGD-specificity of NOTA-Galacto-RGD₂, DOTA-Galacto-RGD₂ and DOTA-3P-RGD₂. The IC₅₀ value of c(RGDyK) was almost identical to that obtained in the same in vitro assay [2,3]. The integrin $\alpha_v\beta_3$ binding affinity of NOTA-Galacto-RGD₂, DOTA-Galacto-RGD₂ and DOTA-3P-RGD₂ was comparable within experimental errors in the same displacement assay.

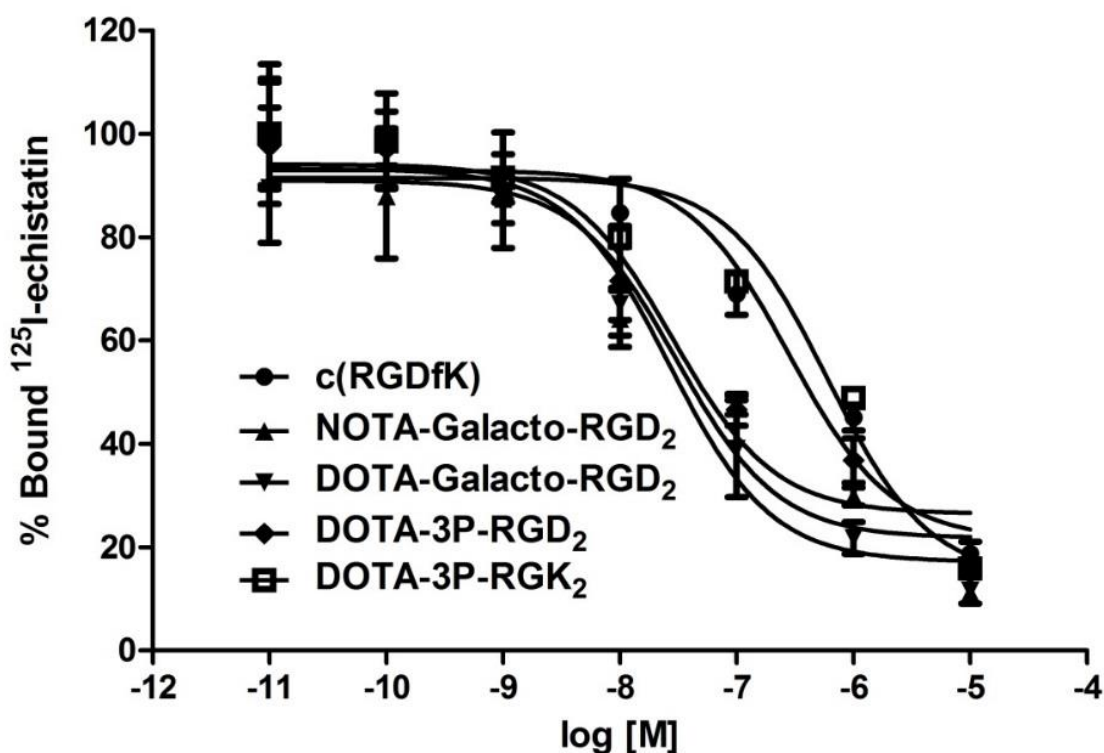


Figure 8. The competitive displacement curves of ^{125}I -echistatin bound to U87MG human glioma cells in the presence of cyclic RGD peptide conjugates. The IC_{50} values were obtained from the curve fitting, and were calculated to be 24 ± 4 , 27 ± 2 , 29 ± 4 , 596 ± 48 and 414 ± 36 nM for NOTA-Galacto-RGD₂, DOTA-Galacto-RGD₂, DOTA-3P-RGD₂, DOTA-Galacto-RGK₂ and c(RGDfK), respectively. c(RGDfK) was used as a standard for the in vitro competitive displacement assay.

Biodistribution.

Figure 9 below lists biodistribution data of ^{111}In (DOTA-Galacto-RGD₂) in athymic nude mice bearing MDA-MB-435 breast cancer xenografts at 1, 4, 24 and 72 h p.i. The ANOVA test was used for this purpose (GraphPad Prim 5.0, San Diego, CA). The level of significance was set at $p < 0.05$. In order to gather coherent results, biodistribution data of ^{111}In (DOTA-3P-RGD₂) was also obtained in the same animal model (Table 1). As illustrated, the tumor uptake of ^{111}In (DOTA-Galacto-RGD₂) (6.79 ± 0.98 , 6.56 ± 0.56 , 4.17 ± 0.61 and 1.09 ± 0.13 %ID/g at 1, 4, 24 and 72 h p.i., respectively) was almost identical to that of ^{111}In (DOTA-3P-RGD₂) (6.79 ± 0.98 , 6.56 ± 0.56 ,

4.17 ± 0.61 and 1.09 ± 0.13 %ID/g at 1, 4, 24 and 72 h p.i., respectively) over the 72 h study period. There was no significant difference in their lung uptake (Tables 1 and 3) and tumor/lung ratios. ¹¹¹In(DOTA-Galacto-RGD₂) had a faster clearance from blood and muscle (Tables 1 and 3). As a result, the tumor/blood and tumor/muscle ratios of ¹¹¹In(DOTA-Galacto-RGD₂) were significantly higher than those of ¹¹¹In(DOTA-3P-RGD₂). However, its tumor/liver ratios (Figure 9) were significantly lower than that for ¹¹¹In (DOTA-3P-RGD₂) at all four time points.

Figure 10 compares biodistribution data of ¹¹¹In(DOTA-Galacto-RGD₂) and ¹¹¹In(NOTA-Galacto-RGD₂) in athymic nude mice bearing MDA-MB-435 breast cancer xenografts at 1, 4, 24 and 72 h p.i. The tumor uptake of ¹¹¹In(DOTA-Galacto-RGD₂) (6.79 ± 0.98, 6.56 ± 0.56, 4.17 ± 0.61 and 1.09 ± 0.13 %ID/g at 1, 4, 24 and 72 h p.i., respectively) was significantly higher than the one of ¹¹¹In(NOTA-Galacto-RGD₂) (2.76 ± 0.47, 1.70 ± 0.03, 0.79 ± 0.19, 0.34 ± 0.12%ID/g at 1, 4, 24 and 72 h p.i., respectively) over the 72 h study period. Tumor/blood, tumor/muscle, tumor/lung and tumor/liver ratios of ¹¹¹In(NOTA-Galacto-RGD₂) were significantly lower than ¹¹¹In(DOTA-Galacto-RGD₂). The only parameter where ¹¹¹In(DOTA-Galacto-RGD₂) performed better than ¹¹¹In(DOTA-Galacto-RGD₂), was the blood uptake at 1h point.

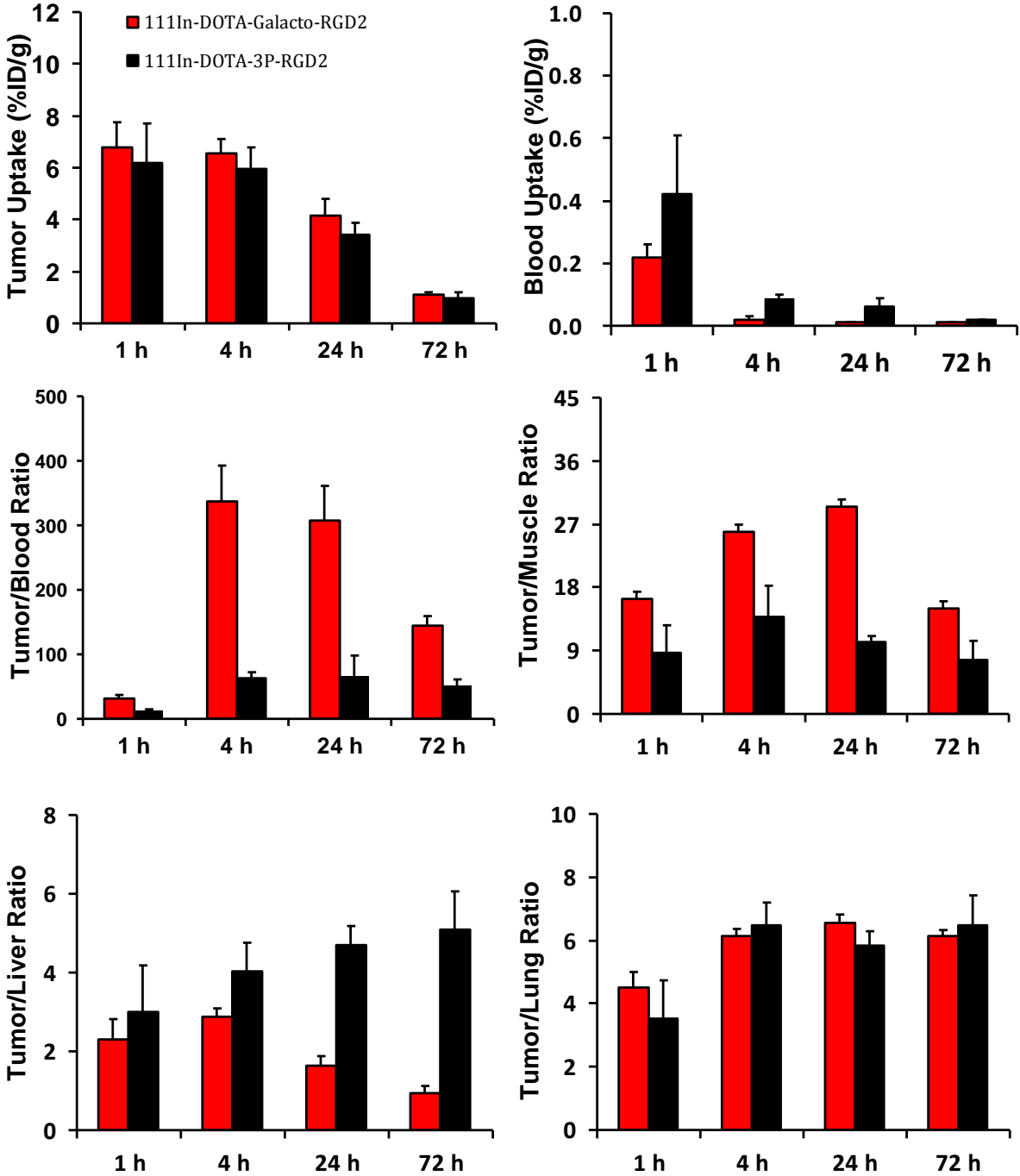


Figure 9. Direct comparison of tumor uptake (% ID/g) and selected tumor/background ratios between ^{111}In (DOTA-Galacto-RGD₂) (n=4) and ^{111}In (DOTA-3P-RGD₂) (n=5) in athymic nude mice bearing MDA-MB-435 human breast cancer xenografts.

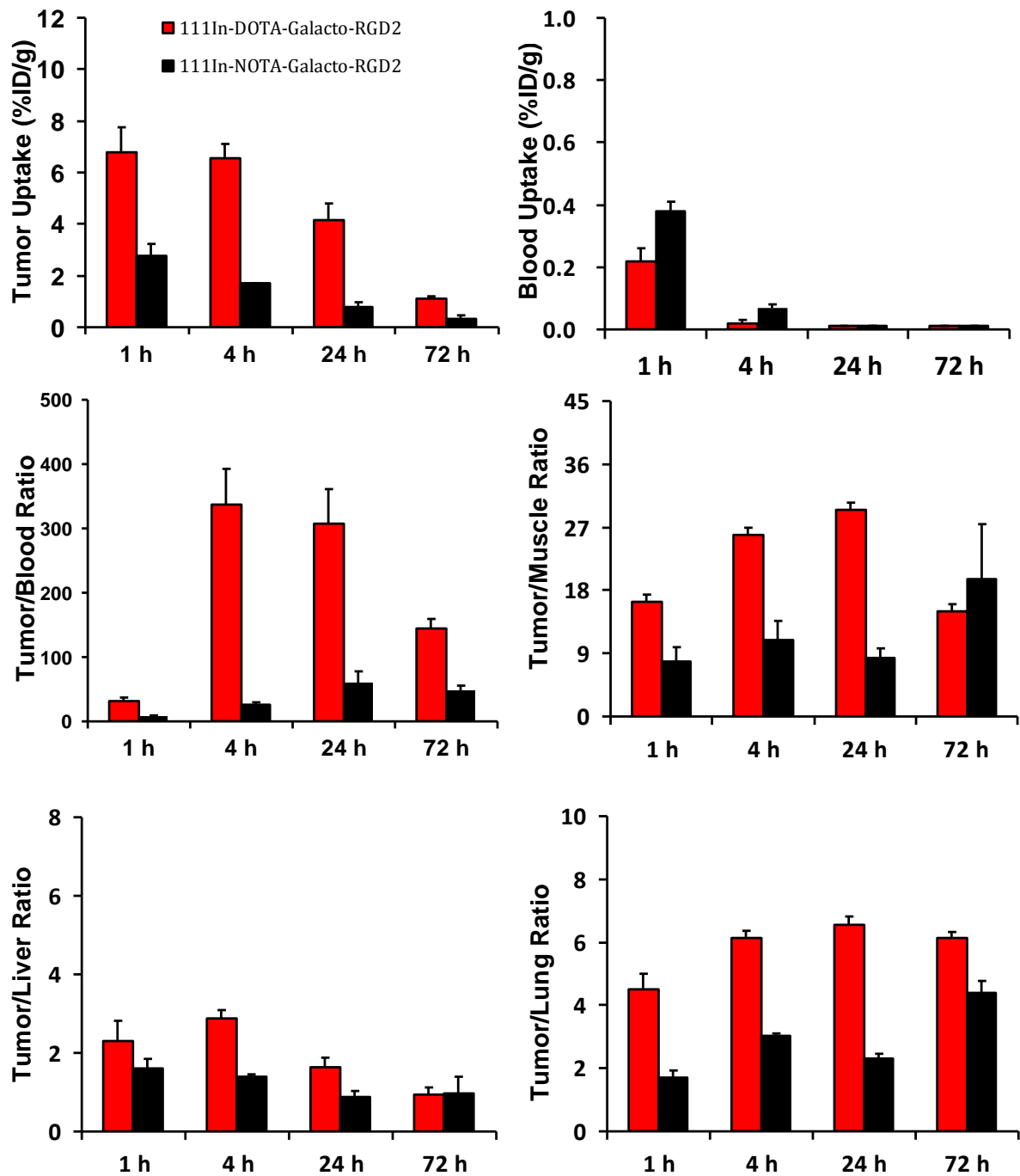


Figure 10. Direct comparison of tumor uptake (% ID/g) and selected tumor/background ratios between ^{111}In (DOTA-Galacto-RGD₂) (n=4) and ^{111}In (NOTA-Galacto-RGD₂) (n=4) in athymic nude mice bearing MDA-MB-435 human breast cancer xenografts.

Planar Imaging.

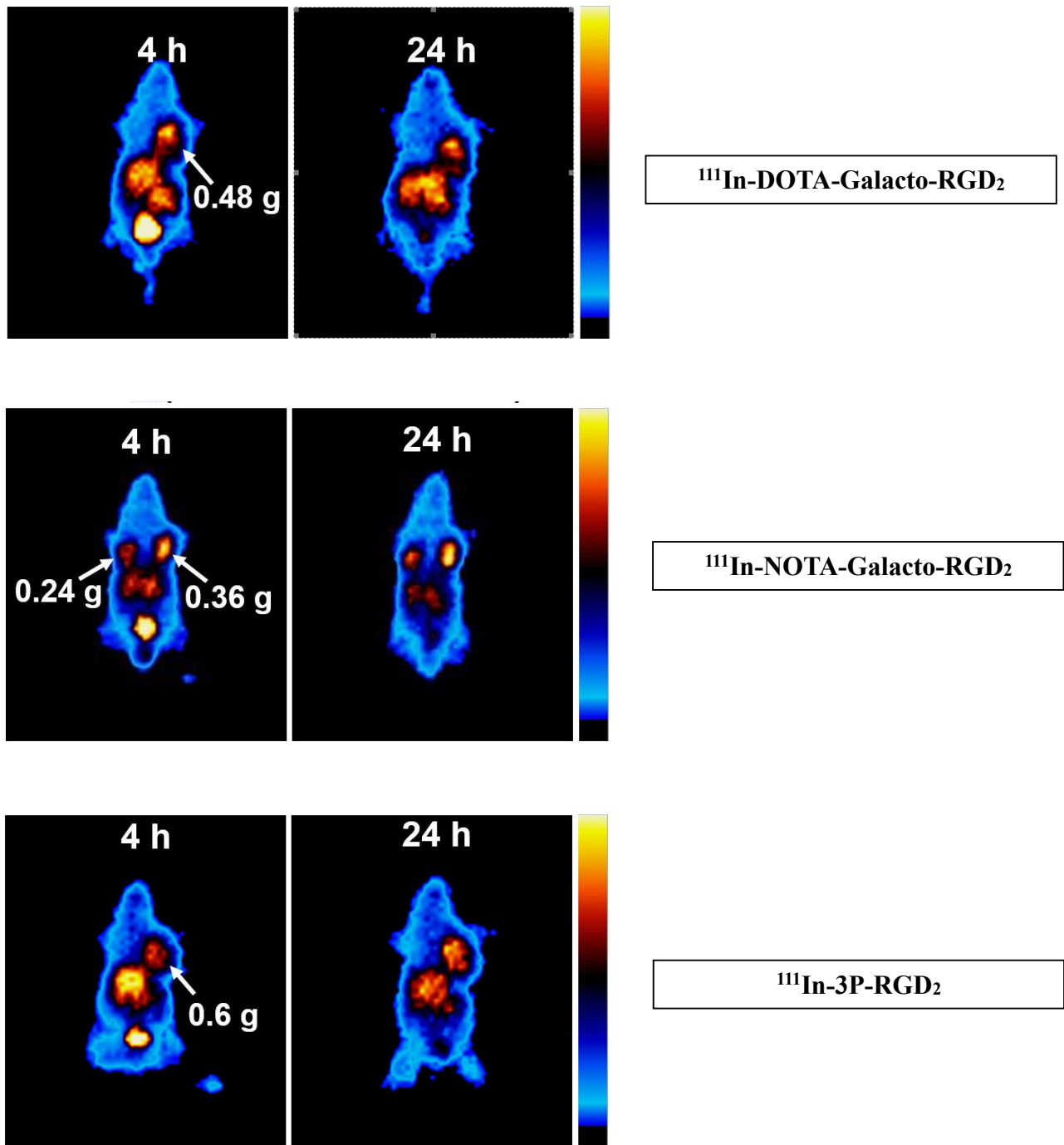


Figure 11. Whole-body planar images of a tumor-bearing mouse administered with 100 μCi of ^{111}In (DOTA-Galacto-RGD₂), 120 μCi of ^{111}In (NOTA-Bz-Galacto-RGD₂) and 100 μCi of ^{111}In (DOTA-3P-RGD₂).

Figure 11 shows whole-body planar images of the tumor-bearing mice administered with 100 – 120 μCi of $^{111}\text{In}(\text{DOTA-Galacto-RGD}_2)$, $^{111}\text{In}(\text{NOTA-Bz-Galacto-RGD}_2)$ (B) and $^{111}\text{In}(\text{DOTA-3P-RGD}_2)$ (C) at 4 and 24 h p.i.

Breast tumors were all clearly visualized with excellent contrast for all three radiotracers. No significant radioactivity enrichment was detected in blood, lungs and muscle. By 24 h, the radioactivity accumulation was detected only in tumors, liver and intestines, which was in agreement with biodistribution data (Tables 1 – 3). Therefore, it is reasonable to believe that $^{111}\text{In}(\text{DOTA-Galacto-RGD}_2)$, $^{111}\text{In}(\text{NOTA-Bz-Galacto-RGD}_2)$ and $^{111}\text{In}(\text{DOTA-3P-RGD}_2)$ are all useful for imaging xenografted MDA-MB-435 breast tumors.

Tumor Tissue Immunohistochemistry and Cellular Immunostaining

We also examined integrin $\alpha_v\beta_3$ expression patterns of MDA-MB-435 cells and the xenografted MDA-MB-435 breast tumor (Figure 12). It was found that integrin $\alpha_v\beta_3$ was expressed mainly on MDA-MB-435 cells with a low expression level of integrin $\alpha_v\beta_3$ on tumor neovasculature. The MDA-MB-435 tumor cells contributed to a major part of integrin $\alpha_v\beta_3$ expression and the tumor uptake of ^{111}In -labeled cyclic RGD peptides. We also found that integrin $\alpha_v\beta_3$ expression on MDA-MB-435 tumors was lower than that reported for the xenografted U87MG glioma which is consistent with the significantly lower uptake of $^{111}\text{In}(\text{DOTA-3P-RGD}_2)$ in MDA-MB-435 breast tumor than U87MG glioma over 72 h study period [170]. Negative control was incubated only with the secondary antibody. This is essential to guarantee specific, reliable coloring. In fact, the cell could not stain if incubated alone with the secondary antibody. The color in the picture indicates so the present of the antigen that was be recognized specifically by the first antibody.

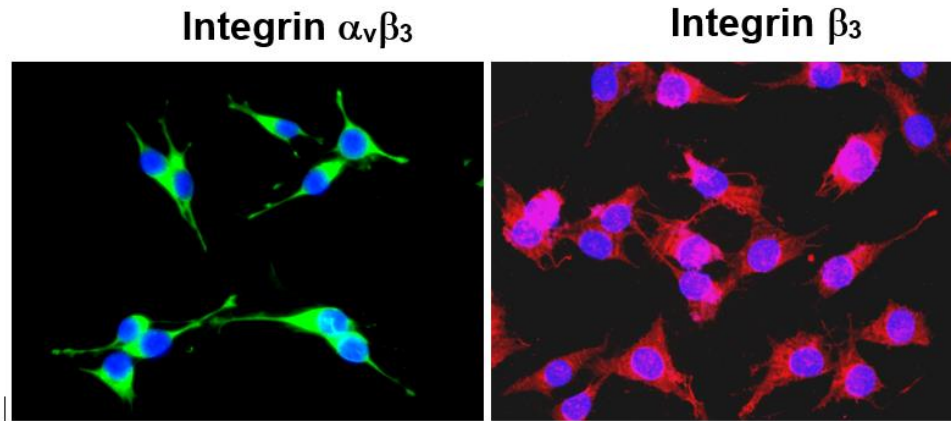


Figure 12. Selected microscopic images (Magnification: 200x) of MDA-MB-435 cells stained with anti-integrin $\alpha_v\beta_3$ (green) and anti-integrin β_3 (red) antibodies. After fixation, cells were washed with PBS, and incubated with Alexa Fluor 488-conjugated mouse anti-human integrin $\alpha_v\beta_3$ antibody LM609 for 1 h, or with rabbit anti-human integrin β_3 antibody followed by incubation with Alexa Fluor 594 conjugated goat anti-rabbit IgG. The blue color indicates the nuclei (DAPI).

Tumor Tissue Histochemistry

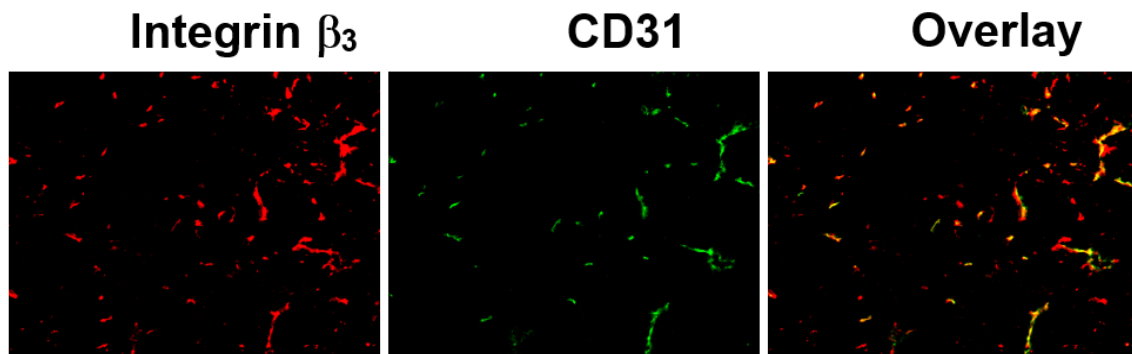


Figure 13. Selected microscopic fluorescence images the tumor slice stained with anti-integrin β_3 (red color) or anti-CD31 (green color) antibody. After fixation, the tissues were incubated with hamster anti-integrin β_3 and rat anti-CD31 antibodies for 1 h followed by incubation with Cy3-conjugated goat anti-hamster and FITC-conjugated goat anti-rat secondary antibodies. Yellow color (red integrin β_3 merged with green CD31) indicates the presence of integrin $\alpha_v\beta_3$ on tumor neo-vasculature.

Integrin $\alpha_v\beta_3$ Specificity.

In order to demonstrate the integrin $\alpha_v\beta_3$ specificity of ^{111}In radiotracers, we carried out two blocking experiments. In the first experiment, ^{111}In (DOTA-Galacto-RGD₂) was used as radiotracer and RGD₂ as blocking agent (~14 mg/kg or ~350 μg per tumor-bearing mouse). Figure 13 shows whole-body planar images of the tumor-bearing mice administered with ~120 μCi of ^{111}In (DOTA-Galacto-RGD₂) in the absence/presence of excess RGD₂ (350 $\mu\text{g}/\text{mouse}$ or 14 mg/kg). In the absence of excess RGD₂, tumor was clearly visualized. In the presence of excess RGD₂, radioactivity accumulation in the breast tumor was almost invisible. In the second experiment, we obtained 60-min biodistribution data of ^{111}In (DOTA-3P-RGD₂) (Table 6) in the athymic nude mice (n = 5) bearing MDA-MB-435 breast cancer xenografts in the absence/presence of RGD₂ (350 $\mu\text{g}/\text{mouse}$ or 14 mg/kg). Co-injection of excess RGD₂ significantly blocked its tumor uptake (0.88 ± 0.08 %ID/g with RGD₂ vs. 6.17 ± 1.56 %ID/g without RGD₂). The normal organ uptake was also blocked by co-injection of excess RGD₂. For example, the uptake of ^{111}In (DOTA-Galacto-RGD₂) in intestine, lungs and spleen was 4.08 ± 1.44 , 1.58 ± 0.26 , and 1.44 ± 0.20 %ID/g, respectively, without RGD₂, while its uptake in the same organs was 1.63 ± 0.31 , 0.37 ± 0.05 , and 0.21 ± 0.07 %ID/g, respectively, in the presence of excess RGD₂.

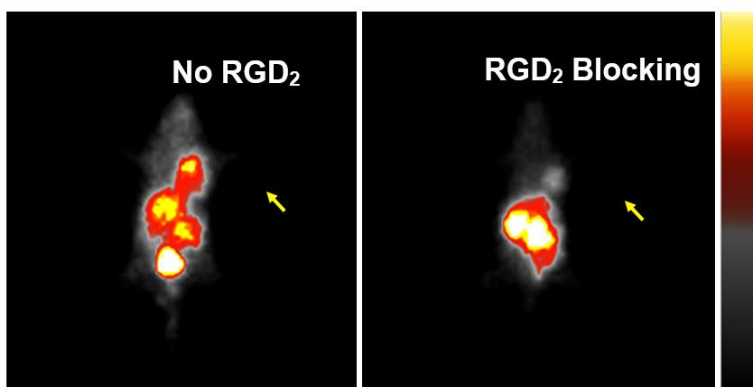


Figure 13. Whole-body planar images of tumor-bearing mice administered with ~100 μCi of ^{111}In (DOTA-Galacto-RGD₂) at 4 h p.i. without (left) /with (right) co-injection of RGD₂ (350 $\mu\text{g}/\text{mouse}$ or 14 mg/kg). The arrow points to the visualized (left) and hidden (right) tumor.

These results clearly demonstrated that the uptake of $^{111}\text{In}(\text{DOTA-Galacto-RGD}_2)$ in tumors and some normal organs is indeed integrin $\alpha_v\beta_3$ -specific.

$^{111}\text{In}(\text{DOTA-3P-RGK}_2)$ was prepared to illustrate the RGD-specificity of ^{111}In -labeled cyclic RGD peptides. The arrow indicates the presence of the visible tumor in the left image acquired after injection of $^{111}\text{In}(\text{DOTA-Galacto-RGD}_2)$. In the right image, acquire after co-injection of RGD_2 and radiotracer, the tumor can no longer be detected. The main activity is to see in the bladder, which implies a high renal excretion.

RGD Specificity.

To demonstrate the RGD-specificity of ^{111}In cyclic RGD peptides, we obtained the 60 min biodistribution data of $^{111}\text{In}(\text{DOTA-3P-RGK}_2)$.

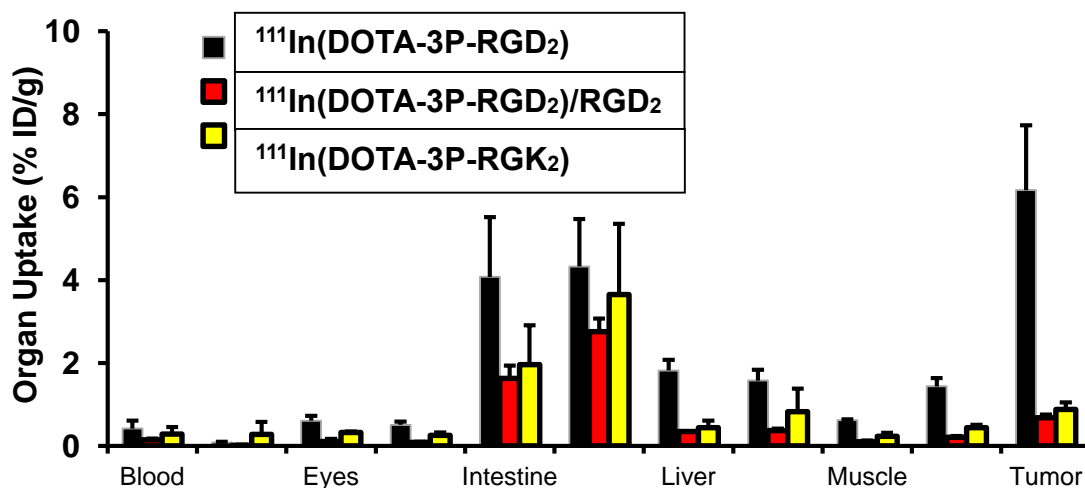


Figure 14. Comparison of biodistribution data of $^{111}\text{In}(\text{DOTA-3P-RGD}_2)$ and $^{111}\text{In}(\text{DOTA-3P-RGK}_2)$ at 60 min p.i. in athymic nude mice ($n = 5$) bearing MDA-MB-435 breast tumor xenografts with/without co-injection of $\text{E}[c(\text{RGDFK})]_2$ (RGD_2 : 350 $\mu\text{g}/\text{mouse}$ or 14 mg/kg).

3P-RGK₂ has identical composition as 3P-RGD₂, but its amino acid sequence was scrambled. Because of very low integrin $\alpha_v\beta_3$ affinity of DOTA-3P-RGK₂ (IC₅₀ = 715 ± 45 nM against 125I-c(RGDyK) bound to U87MG glioma cells) ¹¹¹In(DOTA-3P-RGK₂) had significantly lower (p < 0.01) uptake than ¹¹¹In(DOTA-3P-RGD₂) in both breast tumors and integrin $\alpha_v\beta_3$ -positive normal organs, particularly intestine, liver, lungs and spleen (Figure 14). Despite this the ¹¹¹In-labeled cyclic RGD peptides are RGD-specific. Blocking experiments were used to demonstrate $\alpha_v\beta_3$ specificity. ¹¹¹In(DOTA-3P-RGK₂) was used to illustrate the RGD-specificity of ¹¹¹In radiotracers. When blocked with the 14 mg/kg RGD₂, the uptake of the ¹¹¹In(DOTA-3P-RGD₂) in the blood, eye, heart, intestine, kidney, liver, lung, muscle, spleen was decreased significantly (Figure 14, P < 0.05, one-way ANOVA, Newman-Keuls Test), while the uptake in the tumor was decreased highly significantly (P < 0.01). Compared with ¹¹¹In(DOTA-3P-RGD₂), the biodistribution data of ¹¹¹In(DOTA-3P-RGK₂) demonstrated a significantly lower accumulation of the radiotracer in the intestine, liver and spleen (P < 0.05). The tumor uptake of ¹¹¹In(DOTA-3P-RGD₂) was also significantly much lower than ¹¹¹In(DOTA-3P-RGD₂) (P < 0.01).

4. Discussion

In this study, we evaluated $^{111}\text{In}(\text{DOTA-Galacto-RGD}_2)$, $^{111}\text{In}(\text{NOTA-Galacto-RGD}_2)$ and $^{111}\text{In}(\text{DOTA-3P-RGD}_2)$ as integrin $\alpha_v\beta_3$ -targeted radiotracers for breast tumor imaging. The results from an in vitro displacement assay showed that replacing PEG₄ groups in 3P-RGD₂ with a pair of SAA, 1,2,3-triazole and PEG₂ moieties had no significant change in integrin $\alpha_v\beta_3$ binding affinity (Figure 8) with IC₅₀ of 24±4 nM for DOTA-Galacto-RGD, 27±2 nM for DOTA-Galacto-RGD₂, and 29±4 nM for DOTA-3P-RGD₂. This explains why $^{111}\text{In}(\text{DOTA-Galacto-RGD}_2)$ and $^{111}\text{In}(\text{DOTA-3P-RGD}_2)$ shared almost identical tumor uptake over the 72 h period (Figure 9A). Planar imaging results suggest that $^{111}\text{In}(\text{DOTA-Galacto-RGD}_2)$, $^{111}\text{In}(\text{NOTA-Galacto-RGD}_2)$ and $^{111}\text{In}(\text{DOTA-3P-RGD}_2)$ are all good SPECT radiotracers with a long tumor retention. The integrin $\alpha_v\beta_3$ specificity of $^{111}\text{In}(\text{DOTA-Galacto-RGD}_2)$ was clearly demonstrated by blocking experiments (Figure 13). The RGD specificity was illustrated by comparing biodistribution characteristics of $^{111}\text{In}(\text{DOTA-3P-RGD}_2)$ and $^{111}\text{In}(\text{DOTA-3P-RGK}_2)$ in the same tumor-bearing animal model (Figure 14). The relatively low integrin $\alpha_v\beta_3$ expression level on MDA-MB-435 breast tumors was compared with that one on U87MG glioma and it was consistent by showing a lower uptake of $^{111}\text{In}(\text{DOTA-3P-RGD}_2)$ in MDA-MB-435 breast tumor than U87MG glioma over 72 h study period [136, 138].

According to the results we believe that $^{111}\text{In}(\text{DOTA-Galacto-RGD}_2)$, $^{111}\text{In}(\text{NOTA-Galacto-RGD}_2)$ and $^{111}\text{In}(\text{DOTA-3P-RGD}_2)$ are all suitable SPECT radiotracers for breast cancer imaging and they can all be successfully used for noninvasive monitoring of the tumor integrin $\alpha_v\beta_3$ expression. The difference between $^{111}\text{In}(\text{DOTA-Galacto-RGD}_2)$ and $^{111}\text{In}(\text{DOTA-3P-RGD}_2)$ is that the two PEG₄ groups between two cyclic RGD moieties in 3P-RGD₂ are replaced with a pair of SAA, 1,2,3-triazole and PEG₂ moieties. Even though $^{111}\text{In}(\text{DOTA-Galacto-RGD}_2)$ and

$^{111}\text{In}(\text{DOTA-3P-RGD}_2)$ share very similar biodistribution characteristics (tables 1 and 2), $^{111}\text{In}(\text{DOTA-Galacto-RGD}_2)$ had as hoped a faster washout from blood and muscle than $^{111}\text{In}(\text{DOTA-3P-RGD}_2)$ (Figure 9A). On the other side its tumor/liver ratios are disadvantageous because they are lower than those of $^{111}\text{In}(\text{DOTA-3P-RGD}_2)$ (Figure 9A). For diagnostic radiotracers, the contrast between targeted organ (such as tumor) and surrounding tissues is critically important. As long as the linker between cyclic RGD moieties is long enough to maintain the bivalency, incorporation of more hydrophilic groups (such as SAA and 1,2,3-triazole) is a viable approach to improve radiotracer excretion kinetics from normal organs, such as blood, liver, lungs and muscle. This conclusion is completely consistent with the published results for [^{18}F]-Galacto-RGD and ^{18}F -RGD-K5 [165, 166, 167-169]. Reduction of radioactivity accumulation in the blood and muscle is important to maximize the T/B ratios of radiotracers.

It seems that metal chelates ($^{111}\text{In}(\text{DOTA})$ vs. [$^{99\text{m}}\text{Tc}(\text{HYNIC})(\text{tricine})(\text{TPPTS})$]) also have significant effects on biodistribution properties of their radiotracers. For example, $^{111}\text{In}(\text{DOTA-Galacto-RGD}_2)$ has lower uptake than $^{99\text{m}}\text{Tc-Galacto-RGD}$ in most normal organs except liver and spleen [142]. This difference is likely to be caused by the negatively charged TPPTS, which may interact with positively charged proteins, such as albumin, as shown by higher blood radioactivity accumulation for $^{99\text{m}}\text{Tc-Galacto-RGD}_2$ than that of $^{111}\text{In}(\text{DOTA-Galacto-RGD}_2)$. $^{111}\text{In}(\text{DOTA})$ is neutral and highly hydrophilic and has as such a faster excretion, lower background radioactivity and higher T/B ratios for $^{111}\text{In}(\text{DOTA-Galacto-RGD}_2)$. The high-tumor uptake of the compound can be demonstrated by comparing biodistribution data with the one of previously studied RGD such as $^{99\text{m}}(\text{HYNIC})\text{-RGD}$. $^{111}\text{In}(\text{DOTA-Galacto-RGD}_2)$ has a tumor uptake of 6.79 ± 0.98 after 1h and 6.56 ± 0.56 after 4h while $^{99\text{m}}(\text{HYNIC})\text{-RGD}$ has an uptake of 2.73 ± 0.26 after 1h and 2.06 ± 0.37 after 4h [171]. Despite the differences in animal and tumor models between the two

studies that must be taken in consideration, the tumor uptake of ^{111}In -DOTA-Galacto-RGD₂ looks promising.

It has been demonstrated that many normal organs (particularly intestine, liver, lung, kidneys and spleen) are integrin $\alpha_v\beta_3$ -positive [138]. This is consistent with the reduced uptake of ^{111}In (DOTA-3P-RGD₂) in these organs (Figure 14) in the presence of excess RGD₂. However, this does not mean that the radioactivity accumulation in these organs is only based on integrin $\alpha_v\beta_3$ -binding. Other chemical and non specific binding components play a significant role as well. This is confirmed by the fact that replacing a bulky and negatively charged [$^{99\text{m}}\text{Tc}$ (HYNIC)(tricine)(TPPTS)] with a smaller and highly hydrophilic ^{111}In (DOTA) resulted in lower background radioactivity and higher tumor-to-background ratios for ^{111}In (DOTA-Galacto-RGD₂). ^{111}In (DOTA-3P-RGK₂) has very low integrin $\alpha_v\beta_3$ binding affinity ($\text{IC}_{50} = 715.8 \pm 45.1$ nM) but it still shows a significant uptake in intestine, lung, kidneys and spleen [139] (Figure 14). Co-administration of RGD₂ reduced the uptake of ^{111}In (DOTA-3P-RGD₂) in intestine, liver and lungs by only 60 – 70% of its origin value. The remaining portions of radioactivity accumulation in these organs are most likely due to non-specific binding of ^{111}In radiotracers.

5. Conclusion

In this study, we found that the integrin $\alpha_v\beta_3$ affinity of DOTA-Galacto-RGD₂ was almost identical to the one of DOTA-3P-RGD₂. ¹¹¹In(DOTA-Galacto-RGD₂) and ¹¹¹In(DOTA-3P-RGD₂) shared a similar tumor uptake over 72 h period. We demonstrated that their tumor-uptake is integrin $\alpha_v\beta_3$ and RGD specific. Even though ¹¹¹In(DOTA-Galacto-RGD₂) has a positive faster washout from blood and muscle than ¹¹¹In(DOTA-3P-RGD₂) due to the introduction of the hydrophilic linkers, its tumor/liver ratios are not promising since they are much lower than those of ¹¹¹In(DOTA-3P-RGD₂). Planar imaging data suggest that ¹¹¹In(DOTA-Galacto-RGD₂) and ¹¹¹In(NOTA-Bz-Galacto-RGD₂) are all suitable SPECT radiotracers for imaging integrin $\alpha_v\beta_3$ -positive breast tumors and related metastases. We proved this by comparing their planar images with the one of ¹¹¹In(DOTA-3P-RGD₂), a previously studied, excellent integrin $\alpha_v\beta_3$ radiotracer. The result of biodistribution studies are not compatible with the one from the planar images. In fact, in our biodistribution studies the tumor uptake of ¹¹¹In(NOTA-Bz-Galacto-RGD₂) was significantly lower than the one of ¹¹¹In(DOTA-Galacto-RGD₂). From the overall results, we were not able to prove that ¹¹¹In(NOTA-Bz-Galacto-RGD₂) is an efficient radiotracer for clinical use in cancer diagnosis yet. We chose to use NOTA as a chelator together with the ¹¹¹In even though this is quite unusual. Compared with DOTA, NOTA have the advantage that the labeling can be performed at room temperature. We aimed to produce ¹¹¹In-NOTA-RGD peptides as an intermediate step in the development of ¹⁸F-NOTA-RGD-peptides, which would have a promising clinical impact since the isotope ¹⁸F is nowadays one of most utilized. The time at Purdue University was not long enough for me to work on ¹¹¹In(NOTA-Bz-Galacto-RGD₂) but further research must be carried out. A labeling with a different isotope such as ⁶⁸Ga could be a further strategic approach. In fact, NOTA is well known for its high chemical stability in complexes with

^{68}Ga or ^{64}Cu [172]. Moreover, gallium-NOTA complex [173, 174] have a high symmetry octahedral coordination geometry and an excellent thermodynamic stability as compared to gallium-DOTA complex [175].

6. Tables

Table 1. Biodistribution data and tumor-to-background ratios of $^{111}\text{In}(\text{DOTA-Galacto-RGD}_2)$ in athymic nude mice (n = 4) bearing MDA-MB-435 breast cancer xenografts. The tumor uptake was expressed as an average plus/minus the standard deviation.

Organ	1 h	4 h	24h	72 h
Blood	0.22 ± 0.04	0.02 ± 0.01	0.01 ± 0.00	0.01 ± 0.000
Brain	0.09 ± 0.02	0.11 ± 0.02	0.13 ± 0.07	0.05 ± 0.02
Eyes	0.45 ± 0.08	0.59 ± 0.27	0.39 ± 0.07	0.12 ± 0.03
Heart	0.77 ± 0.09	0.58 ± 0.22	0.35 ± 0.05	0.18 ± 0.09
Intestine	3.13 ± 0.34	2.36 ± 0.36	1.88 ± 0.33	0.96 ± 0.15
Kidneys	4.65 ± 0.89	3.13 ± 0.28	3.06 ± 0.28	1.44 ± 0.23
Liver	3.01 ± 0.36	2.29 ± 0.20	2.58 ± 0.42	1.20 ± 0.13
Lungs	1.61 ± 0.33	1.23 ± 0.54	0.65 ± 0.12	0.23 ± 0.11
Muscle	0.45 ± 0.13	0.26 ± 0.05	0.15 ± 0.04	0.08 ± 0.03
Spleen	1.77 ± 0.14	1.47 ± 0.49	1.34 ± 0.31	0.67 ± 0.15
Tumor	6.79 ± 0.98	6.56 ± 0.56	4.17 ± 0.61	1.09 ± 0.13
Tumor/Blood	31.62 ± 5.18	336.87 ± 55.98	307.61 ± 53.58	144.04 ± 15.60
Tumor/Liver	2.31 ± 0.50	2.87 ± 0.22	1.64 ± 0.24	0.93 ± 0.19
Tumor/Lung	4.50 ± 1.62	6.15 ± 1.98	6.56 ± 1.13	6.13 ± 3.28
Tumor/Muscle	16.44 ± 5.20	25.95 ± 4.76	39.46 ± 3.93	15.06 ± 7.25

Table 2. Selected biodistribution data of $^{111}\text{In}(\text{DOTA-3P-RGD}_2)$ in the athymic nude mice ($n = 5$) bearing MDA-MB-435 breast cancer xenografts. The tumor uptake was expressed as an average plus/minus the standard deviation from 5 tumor-bearing animals.

%ID/gram	1 h	4 h	24 h	72 h
Blood	0.42 ± 0.19	0.09 ± 0.01	0.06 ± 0.03	0.02 ± 0.00
Brain	0.08 ± 0.02	0.06 ± 0.01	0.04 ± 0.01	0.02 ± 0.00
Eyes	0.61 ± 0.12	0.44 ± 0.07	0.27 ± 0.03	0.14 ± 0.01
Heart	0.51 ± 0.08	0.31 ± 0.08	0.23 ± 0.07	0.08 ± 0.00
Intestine	4.08 ± 1.44	3.32 ± 0.79	3.15 ± 1.71	0.92 ± 0.45
Kidneys	4.33 ± 1.14	2.61 ± 0.48	1.84 ± 0.47	0.72 ± 0.05
Liver	1.82 ± 0.26	1.50 ± 0.32	0.70 ± 0.13	0.20 ± 0.04
Lungs	1.58 ± 0.26	0.92 ± 0.11	0.56 ± 0.14	0.16 ± 0.03
Muscle	0.62 ± 0.02	0.48 ± 0.22	0.32 ± 0.03	0.14 ± 0.03
Spleen	1.44 ± 0.20	1.10 ± 0.27	0.84 ± 0.02	0.35 ± 0.10
MDA-MB-435	6.17 ± 1.56	5.94 ± 0.84	3.40 ± 0.50	0.99 ± 0.20
Tumor/Blood	12.25 ± 3.13	63.66 ± 8.14	67.52 ± 30.85	51.25 ± 9.02
Tumor /Liver	3.00 ± 1.18	4.03 ± 0.72	4.71 ± 0.47	5.10 ± 0.95
Tumor /Lung	3.54 ± 1.57	6.47 ± 0.67	5.82 ± 0.26	6.46 ± 1.87
Tumor /Muscle	8.73 ± 3.84	13.75 ± 4.55	10.31 ± 0.84	7.64 ± 2.83

Table 3. Biodistribution data and tumor-to-background ratios of $^{111}\text{In}(\text{NOTA-Bz-Galacto-RGD}_2)$ in athymic nude mice (n = 4) bearing MDA-MB-435 breast cancer xenografts. The tumor uptake was expressed as an average plus/minus the standard deviation.

Organ	1 h	4 h	24h	72 h
Blood	0.38 ± 0.03	0.07 ± 0.01	0.01 ± 0.00	0.01 ± 0.000
Brain	0.08 ± 0.01	0.06 ± 0.04	0.02 ± 0.01	0.01 ± 0.000
Eyes	0.78 ± 0.21	0.20 ± 0.04	0.15 ± 0.08	0.06 ± 0.06
Heart	0.64 ± 0.10	0.22 ± 0.03	0.15 ± 0.02	0.09 ± 0.06
Intestine	2.15 ± 0.34	0.76 ± 0.07	0.48 ± 0.08	0.22 ± 0.09
Kidneys	10.95 ± 0.85	6.89 ± 0.55	4.48 ± 0.46	1.70 ± 0.89
Liver	1.72 ± 0.21	1.23 ± 0.08	0.91 ± 0.12	0.41 ± 0.20
Lungs	1.64 ± 0.16	0.56 ± 0.05	0.35 ± 0.01	0.13 ± 0.08
Muscle	0.36± 0.04	0.17 ± 0.04	0.10 ± 0.03	0.02 ± 0.01
Spleen	1.04 ± 0.22	0.69 ± 0.09	0.52 ± 0.11	0.41 ± 0.29
Tumor	2.76± 0.47	1.70 ± 0.03	0.79 ± 0.19	0.34 ± 0.12
Tumor/Blood	7.34± 1.47	26.38 ± 3.42	59.56 ±18.55	47.30 ± 8.97
Tumor/Liver	1.61 ± 0.25	1.39 ±0.07	0.87± 0.16	0.98 ± 0.40
Tumor/Lung	1.70 ± 0.32	3.04 ± 0.22	2.30 ±0.56	4.38 ± 3.48
Tumor/Muscle	7.88 ± 1.94	10.88±2.68	8.27 ± 1.42	19.58 ± 7.94

Table 4. The body weight of atymic nude mice after injection of tumor cells measured by electric balance. (g)

<i>Mouse nr./days</i>	6	7	8	10	11	13	14	15
1	20.4	19.8	19.6	19.7	19.4	20.0	20.4	20.5
2	22.5	22.5	22.6	24.4	22.4	22.8	22.8	22.8
3	22.5	22.2	22.3	21.6	23.4	22.5	22.1	22.6
4	20.6	20.6	20.7	20.7	19.0	20.5	20.6	20.9
5	24.3	22.9	22.9	23.7	23.7	24.5	24.2	24.6
6	21.1	20.8	20.6	21.4	21.0	21.4	21.2	21.7
7	22.3	22.3	22.5	22.1	22.1	22.9	22.7	23.2
8	22.6	22.2	21.6	22.4	22.4	22.8	22.8	23.3
9	21.4	21.9	21.7	21.8	21.2	21.6	21.9	22.2
10	21.7	20.1	22.3	21.3	21.4	22.0	21.5	21.9
11	19.9	21.5	20.5	19.5	19.3	20.1	19.5	20.4
12	23.1	23.1	23.3	23.1	20.6	22.8	22.5	23.3
13	21.3	21.3	20.6	20.1	20.3	20.5	20.9	20.7
14	25.8	25.4	25.4	25.5	25.2	25.8	25.3	26.0
15	20.9	20.5	20.3	20.6	22.9	20.9	20.0	21.3
16	21.1	21.3	21.0	21.2	21.0	21.5	21.5	21.8
17	23.5	23.0	23.8	24.5	24.3	24.7	24.3	25.0
mean	22.1	21.8	21.9	22.0	21.7	22.2	22.0	22.5
sd	1.5	1.3	1.4	1.7	1.7	1.6	1.5	1.6

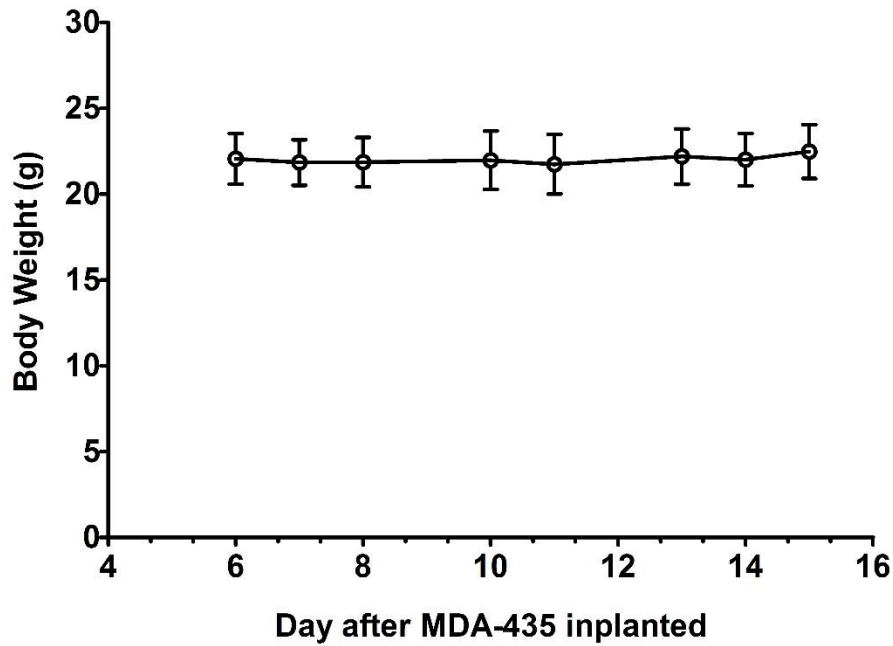


Figure 1. The body weight of the mice bearing MDA-MB-435 at different days after implanted.

Table 5. The tumor volume measured by electric caliper. (mm³)

	6	7	8	10	11	13	14	15
1	16.98	28.48	46.75	64.22	91.30	133.02	141.89	142.46
2	18.18	27.05	39.13	66.23	111.01	124.65	144.86	174.94
3	18.37	16.06	16.62	24.44	28.99	124.62	293.31	344.85
4	14.70	17.59	22.80	48.24	53.80	69.74	126.29	162.45
5	10.15	15.61	22.11	40.58	68.42	133.87	155.72	187.66
6	15.73	19.19	16.64	36.97	61.82	149.33	147.26	190.09
7	6.56	13.94	17.16	44.42	40.17	92.82	94.50	132.81
8	15.97	14.70	39.86	73.74	50.77	110.98	118.33	126.49
9	12.87	11.88	10.68	18.87	15.62	37.92	37.38	33.21
10	42.78	52.89	68.97	144.76	135.88	211.88	226.74	297.51
11	19.54	17.13	24.18	45.74	48.81	93.30	105.22	125.42
12	23.19	21.74	28.05	53.32	36.16	82.12	125.82	152.72
13	28.83	16.34	26.35	30.06	56.61	97.07	76.00	99.54
14	11.04	13.12	9.52	21.79	41.04	107.39	200.76	193.06
15	16.10	12.51	17.87	43.93	46.42	55.83	70.98	92.00
16	46.55	40.80	60.52	91.56	94.02	144.05	182.66	229.43
17	8.99	33.92	40.52	54.63	71.10	108.32	308.80	329.02
mean	19.2	21.9	29.9	53.1	61.9	110.4	150.4	177.3
sd	10.6	11.0	16.5	29.5	30.0	39.0	71.6	81.2

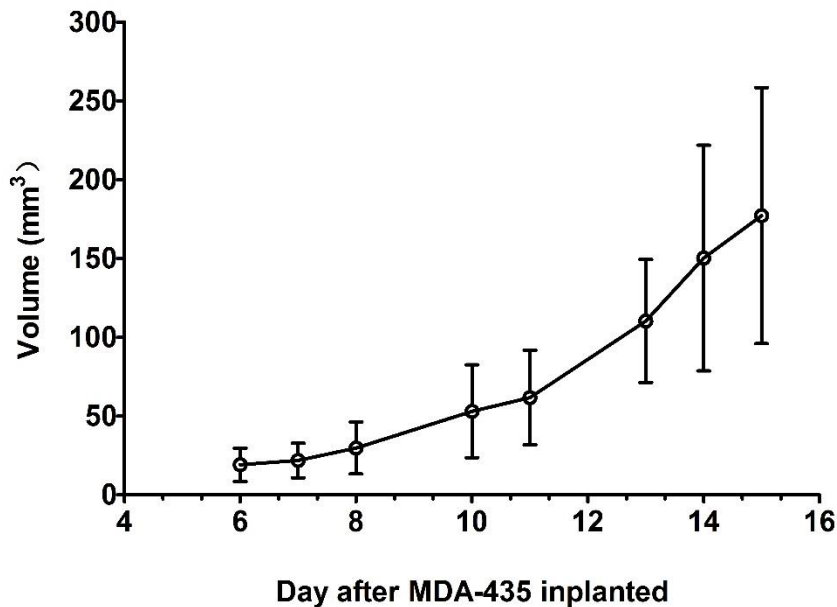


Figure 2. The growth curve of the tumor in mice bearing MDA-MB-435 at different days after implant

7. Annex

Materials and instruments used for the preparation of the Galacto-RGD₂ Peptides.

Chemicals and solvents were purchased from Sigma/Aldrich (St. Louis, MO), and used without further purification. DOTA-OSu (1,4,7,10-tetraazacyclododecane-4,7,10-triacetic acid-1-acetate(N-hydroxysuccinimide)) and SCN-Bz-NOTA (2-(p-thiocyanatobenzyl)-1,4,7-triazacyclononane-1,4,7-triacetic acid) were purchased from Macrocyclics (Dallas, TX). E[c(RGDfK)]₂ (RGD₂), DOTA-3P-RGD₂, DOTA-3P-RGK₂, and Glu[cyclo[Arg-Gly-Asp-D-Phe-Lys(SAA-PEG₂-(1,2,3-triazole)-1-yl-4-methylamide)]]₂ (Galacto-RGD₂) were prepared according to the procedures described in our previous reports [7,10]. The MALDI (matrix assisted laser desorption ionizations) mass spectral data were collected using an Applied Biosystems Voyager DE PRO mass spectrometer (Framingham, MA), the Department of Chemistry, Purdue University. The Boc-protected glutamic acid was purchased from Senn Chemicals (San Diego, CA), and 8-azido-3,6-dioxaoctanoic acid (N₃-PEG₂-OH) was from Peptides International Inc. (Louisville, KY). The protected peptide [cyclo[Arg(Pbf)-Gly-Asp(O*t*Bu)-D-Phe-Lys(SAA)]] (Galacto-RGD) was prepared using the procedure reported in the literature. Sodium succinimidyl 6-(2-(2-sulfonatobenzaldehyde)hydrazono)nicotinate (HYNIC-OSu) was prepared according to the literature method. [^{99m}Tc (HYNIC-3P-RGD₂)(tricine)(TPPTS)] (^{99m}Tc-3P-RGD₂) was prepared using the procedure described in our previous reports [3,12] Na^{99m}TcO₄ was obtained from Cardinal HealthCare® (Chicago, IL). Melting point was determined on a Buchi B-540 melting point apparatus and was uncorrected. Optical rotation was determined on a DIP-370 polarimeter (Jasco, Easton, MD). Thin layer chromatography was performed using Merck F₂₅₄ silica gel plates (EMD, Darmstadt, Germany). NMR spectra were recorded with a Varian Unity 500 Plus spectrometer (Palo Alto, CA) in DMSO-*d*₆.

HPLC Method for Cyclic Galacto RGD peptides.

HPLC Method 1 used a semi-prep LabAlliance HPLC system (Scientific Systems, Inc., State College, PA) equipped with a UV/vis detector ($\lambda=220$ nm) and Zorbax C18 column (9.4 mm x 250 mm, 100 Å pore size; Agilent Technologies, Santa Clara, CA). The flow rate was 2.5 mL/min with a mobile phase being 90% A and 10% B at 0 min to 85%A and 15% B at 5 min, and to 75%A and 25% B at 20 min. Radio-HPLC (Method 2) used the Agilent HP-1100 HPLC system (Agilent Technologies, Santa Clara, CA) equipped with a β -ram IN/US detector (Tampa, FL) and Zorbax C18 column (4.6 mm x 250 mm, 300 Å pore size; Agilent Technologies, Santa Clara, CA). The flow rate was 1 mL/min. The gradient mobile phase started with 90% A (25 mM NH₄OAc, pH = 6.8) and 10% B (acetonitrile) to 85% A and 15% B at 5 min, followed by a gradient mobile phase going from 15% B at 5 min to 20% B at 20 min and to 60% B at 25 min.

Preparation of Boc-L-Glutamic Acid Bis-Propargyl Amide (1)

To a solution of Boc-glutamic acid (2.47 g, 10 mmol) and propargylamine hydrochloride (2.11 g, 23 mmol) in DMF (30 mL) were added diphenylphosphoryl azide (DPPA: 5.2 mL, 24 mmol) and triethylamine (Et₃N, 3.2 mL, 23 mmol) at 0 °C under vigorous stirring. The reaction was allowed to proceed overnight at 0 °C. The pH value of the reaction mixture was kept at 7 ~ 8 with Et₃N. The reaction mixture was taken into EtOAc (500 mL) and washed with 0.2 N HCl (2 x 200 mL), brine (100 mL), saturated NaHCO₃ solution (3 x 200 mL), and brine (2 x 100 mL). After drying over Na₂SO₄, EtOAc was removed to yield 4.16 g of crude product, which upon trituration with hot isopropyl ether afforded a white solid (2.66 g, 82.9 %). R_f (EtOAc/Hexane/AcOH 2:1:0.01) = 0.20, melting point 146.2-146.5°C, $[\alpha]_{D^{25}}$ 10.4° (c = 1,

CHCl₃). ESI-MS: $m/z = 344.2 [M + Na]^+$; $322.2 [M + H]^+$. ¹H NMR (DMSO-*d*₆, chemical shift δ in ppm, and atom labels according to the structure below): δ 8.25 [1H, bt, $J=5.6$ Hz, N(1a)-H], 8.24 [1H, bt, $J=5.6$ Hz, N(5a)-H], 6.88 [1H, d, $J=8.0$ Hz, N(2a)-H], 3.87 [1H, m, C(2)-H], 3.85 [2H, dd, $J=5.6$ Hz, $J=2.3$ Hz, C(1b)-H₂], 3.82 [2H, dd, $J=5.6$ Hz, $J=2.6$ Hz, C(5b)-H₂], 3.10 [1H, t, $J=2.3$ Hz, C(1d)-H], 3.08 [1H, t, $J=2.6$ Hz, C(5d)-H], 2.10 [2H, m, C(4)-H₂], 1.82 [1H, m, C(3)-H₂], 1.67 [1H, m, C(3)-H₂], and 1.37 [9H, s, C(2e)-H₃]. ¹³C NMR (DMSO-*d*₆, chemical shift δ in ppm): 171.5 (C-1), 171.2 (C-5), 155.2 (C-2b), 81.2 (C-1c), 81.1 (C-5c), 78.1 (C-2d), 73.0 (C-5d), 72.9 (C-1d), 53.8 (C-2), 31.6 (C-4), 28.2 (C-2e), 27.9 (C-1b), 27.8 (C3 and C-5b). Anal. Calculated for C₁₆H₂₃N₃O₄: C, 59.80; H, 7.21; N, 13.08. Found: C, 59.78; H, 7.19; N, 13.00.

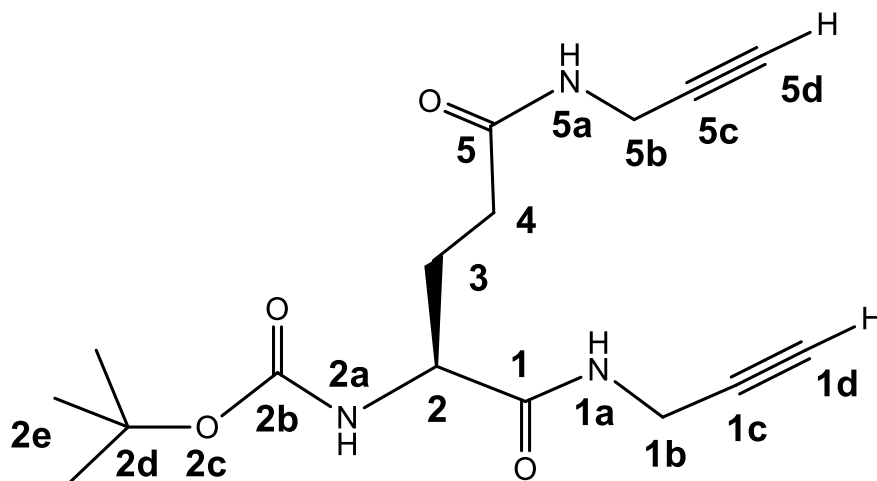


Figure 1. Boc-L-Glutamic Acid Bis-Propargyl Amide

Preparation of Cyclo[Arg(Pbf)-Gly-Asp(OtBu)-D-Phe-Lys(SAA-PEG₂-N₃)]

To a solution of cyclo[Arg(Pbf)-Gly-Asp(OtBu)-D-Phe-Lys(SAA)] (1.10 g, 1.0 mmol) and N₃-PEG₂-OH (0.28 g, 1.48 mmol) in DMF (15 mL) was added DPPA (0.43 mL, 2.0 mmol) at 0 °C with stirring, followed by the addition of Et₃N (0.21 mL, 1.51 mmol). The reaction mixture was

kept at 0 °C for 25 h, with occasional adjustments of the pH (7 – 8), with Et₃N. After the reaction, the mixture was diluted with 0.4 N HCl (100 mL) and extracted with EtOAc (3 x 300 mL). The combined organic extracts were concentrated. The precipitated product was collected by filtration, washed with cold Et₂O, and dried in vacuo to afford 0.81 g of **2** in 63.7 % yield as a colorless solid. ESI-MS: $m/z = 945.55$ [M + H]⁺ (M = 945.43 calcd. for [C₄₀H₅₉N₁₃O₁₄]).

Preparation of Boc-Glu[cyclo[Arg(Pbf)-Gly-Asp(OtBu)-D-Phe-Lys(SAA-PEG₂-(1,2,3-triazole)-1-yl-4-methylamide)]]₂

To a stirred solution of **1** (94 mg, 0.29 mmol) and **2** (750 mg, 0.59 mmol) in a mixture of H₂O (2.9 mL) and *t*-BuOH (5.8 mL) were added 1.73 mL of 0.2 M CuSO₄·5H₂O and 1.73 mL of 0.5 M sodium ascorbate solution at room temperature. The mixture was stirred for 70 min, then diluted with 60 mL *t*-BuOH and 40 mL H₂O. The organic layer was washed with H₂O (2 x 30 mL) and concentrated under reduced pressure. Addition of Et₂O resulted in a precipitate, which was collected by filtration, washed with Et₂O, and dried to give 760 mg of **3**. The yield was 91.5 %. ESI-MS: $m/z = 2249.05$ [M+H]⁺ (M = 2249.05 calcd. for [C₉₆H₁₄₅N₂₉O₃₄]).

Preparation of H-Glu[cyclo[Arg-Gly-Asp-D-Phe-Lys(SAA-PEG₂-(1,2,3-triazole)-1-yl-4-methylamide)]]₂ (Galacto-RGD₂).

The protected Galacto-RGD₂ (750 mg, 0.26 mmol) was dissolved in 20 mL of a solution TFA/TIPS/H₂O (95/2.5/2.5, v/v/v) at room temperature. After 2 h, the reaction mixture was concentrated under reduced pressure. Crude Galacto-RGD₂ was precipitated with cold Et₂O,

collected by centrifugation, washed with Et₂O (3 x 30 mL), and dried in vacuo to give 690 mg of white solid, which was purified by RP-HPLC (Method 1) to yield Galacto-RGD₂ (105 mg, 16.2 %) as a TFA salt. The HPLC purity was 99.3 %. ESI-MS: $m/z = 2149.12$ [M+H]⁺ (M = 2149.05 calcd. for [C₉₁H₁₃₇N₂₉O₃₄]).

Preparation of DOTA-Galacto-RGD₂.

Galacto-RGD₂ (6.5 mg, 3 μmol) and DOTA-OSu (7.5 mg, ~11.0 μmol) were dissolved in 2 mL of dimethylformamide (DMF). After addition of excess diisopropylethylamine (DIEA: 50 μmol), the reaction mixture was stirred for 5 days at room temperature. After addition of water (2 mL), the pH value was adjusted to 3 – 4 with neat TFA. The resulting solution was subjected to HPLC-purification (Method 1). The fraction at ~18 min was collected. Lyophilization of collected fractions afforded DOTA-Galacto-RGD₂. The yield was 4.3 mg (~40%). MALDI-MS (positive mode): $m/z = 2532.45$ for [M + H]⁺ (M = 2534.18 calculated for [C₁₀₇H₁₆₄N₃₃O₃₉]⁺).

Preparation of DOTA-Galacto-RGD₂.

Galacto-RGD₂ (6.5 mg, 3 μmol) and DOTA-OSu (7.5 mg, ~11.0 μmol) were dissolved in 2 mL of dimethylformamide (DMF). After addition of excess diisopropylethylamine (DIEA: 50 μmol), the reaction mixture was stirred for 5 days at room temperature. After addition of water (2 mL), the pH value was adjusted to 3 – 4 with neat TFA. The resulting solution was subjected to HPLC-purification (Method 1). The fraction at ~18 min was collected. Lyophilization of collected fractions afforded DOTA-Galacto-RGD₂. The yield was 4.3 mg (~40%). MALDI-MS (positive mode): $m/z = 2532.45$ for [M + H]⁺ (M = 2534.18 calculated for [C₁₀₇H₁₆₄N₃₃O₃₉]⁺).

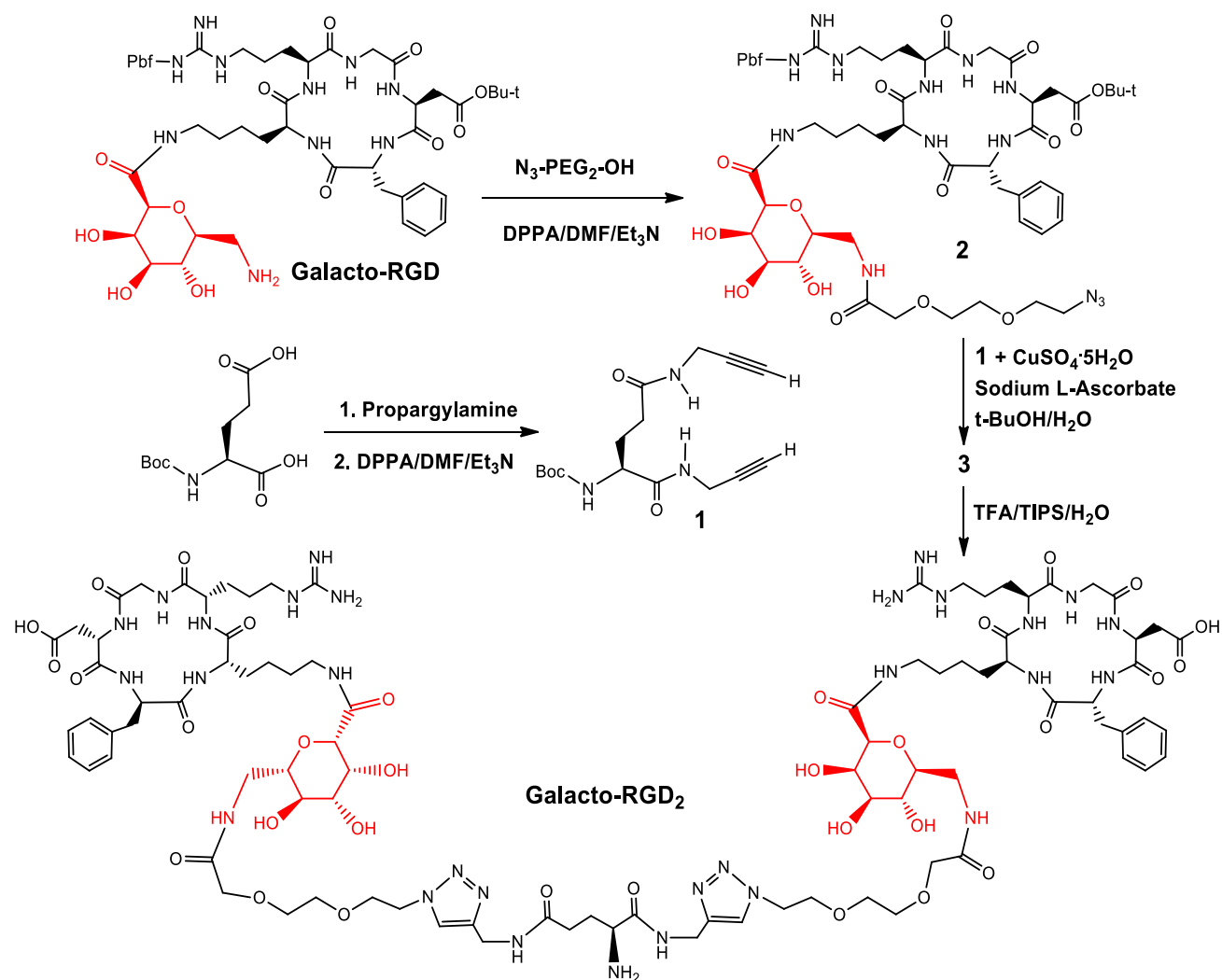


Figure 2. Syntheses of Galacto-RGD₂

Preparation of NOTA-Galacto-RGD₂.

Galacto-RGD₂ (6.5 mg, 3 μmol) and NOTA-Bz-SCN (trichloride salt: 7.5 mg, ~11.0 μmol) were dissolved in 2 mL of anhydrous dimethylformamide (DMF). After addition of excess DIEA (50 μmol), the reaction mixture was stirred for 6 days at room temperature. After addition of water (2 mL), the pH value was adjusted to 3 – 4 with neat TFA. The resulting solution was subjected to HPLC-purification (Method 1). The fraction at ~17 min was collected. Lyophilization of

collected fractions afforded NOTA-Galacto-RGD₂. The yield was 5.6 mg (~40%). MALDI-MS (positive mode): $m/z = 2598.75$ for $[M + H]^+$ ($M = 2598.16$ calculated for $[C_{111}H_{164}N_{33}O_{38}S]^+$).

Result of Synthesis of DOTA-Galacto-RGD₂.

DOTA-Galacto-RGD₂ and NOTA-Galacto-RGD₂ were prepared by reacting DOTA-OSu and NOTA-Bz-NCS, respectively, with Galacto-RGD₂ in the presence of excess DIEA. Completion of conjugation reactions took ~3 days at room temperature. The reaction rate was faster than that between HYNIC-OSu and Galacto-RGD₂ most likely because of higher reactivity of DOTA-OSu and NOTA-Bz-NCS as compared with HYNIC-OSu [16]. DOTA-Galacto-RGD₂ and NOTA-Galacto-RGD₂ were purified by semi-prep HPLC. The MALDI-MS data was consistent with their proposed compositions.

8. References

- (1) I. Dijkgraaf . and C. O. Boerman (2010) Molecular imaging of angiogenesis with SPECT. *Eur J Nucl Med Mol Imag.* 37, 104–113.
- (2) H. E. Daldrup-Link, G. H. Simon and R. C. Brasch (2006) Imaging of Tumor Angiogenesis: Current Approaches and Future Prospects. *Current Pharmaceutical Design.* 12, 2661-2672.
- (3) R. WC. Pang and R. TP. Poon (2006) Clinical Implications of Angiogenesis in Cancer. *Vasc Health Risk Manag* 2, 97-108.
- (4) T. Asahara, H. Masuda, T. Takahashi, C. Kalka, C. Pastore, M. Silver, M. Kearne, JM. Magner Mand Isner (1999) Bone marrow origin of endothelial progenitor cells responsible for postnatal vasculogenesis in physiological and pathological neovascularization. *Circ Research.* 85, 221-228.
- (5) A. B. Peters, A. L. Diaz Jr, K. Polyak, L. Meszler, K. Romans, C. E. Guinan, H. J. Aultin, D. Myerson , R. S. Hamilton, B. Vogelstein, W. K. Kinzler and C. Lengauer (2005) Contribution of bone marrow-derived endothelial cells to human tumor vasculature. *Nat Med.* 11, 261 – 262.
- (6) R. Nasu, H. Kimura, K. Akagi, T. Murata and Y. Tanaka(1999) Blood flow influences vascular growth during tumor angiogenesis. *Br J Cancer.* 79, 780-786.
- (7) J. Rak, RS. K. Sunnybrook (1998) Basic fibroblast growth factor and the complexity of tumor angiogenesis. *Expert Opin Investig Drugs.* 7, 797-801.
- (8) M. Aumailley, M. Gurrath, G. Müller, J. Calvete, R. Timpl, H. Kessler (1991) Arg-Gly-Asp constrained within cyclic pentapeptides. Strong and selective inhibitors of cell adhesion to vitronectin and laminin fragment P1. *FEBS Lett* 291, 50–4.
- (9) M. Janssen, W.J. Oyen, L.F. Massuger, C. Frielink, I. Dijkgraaf, D.S. Edwards, M.

- Radjopadhye, F.H. Corstens, O.C. Boerman (2002) Comparison of a monomeric and dimeric radiolabeled RGD-peptide for tumor targeting. *Cancer Biother. Radiopharm.* 17, 641–646.
- (10) X. Chen, S. Liu, Y. Hou, M. Tohme, R. Park, J.R. Bading, P.S. Conti (2004) MicroPET imaging of breast cancer α_v -integrin expression with ^{64}Cu -labeled dimeric RGD peptides. *Mol. Imaging Biol.* 6, 350–359.
- (11) E. Keshet and S. A. Ben-Sasson (1999) Anticancer drug targets: approaching angiogenesis. *J Clin Invest.* 104, 1497–1501.
- (12) F. Blasi and P. Carmeliet (2002) uPAR: a versatile signaling orchestrator. *Nature Rev. Mol. Cell Biol.* 3, 932–943.
- (13) B.P. Eliceiri and D.A. Cheresh (1998) The role of α_v integrins during angiogenesis. *Mol Med* 4, 741–750.
- (14) R.O. Hynes, B.L. Bader and K. Hodivala-Dilke (1999) Integrins in vascular development. *Braz J Med Biol Res* 32, 501-510.
- (15) M.S. Pepper (2001) Role of the matrix metalloproteinase and plasminogen activator-plasmin systems in angiogenesis. *Arterioscler Thromb Vasc Biol.* 21, 1104-1117.
- (16) S. Liu, W.Y. Hsieh, Y. Jiang, Y.S. Kim, S.G. Sreerama, X. Chen et al. (2007) Evaluation of a $^{99\text{m}}\text{Tc}$ -labeled cyclic RGD tetramer for noninvasive imaging integrin $\alpha_v\beta_3$ -positive breast cancer. *Bioconjug Chem.* 18, 438–46.
- (17) J. Yang, H. Guo, F. Gallazzi, M. Berwick, R.S. Padilla, Y. Miao (2009) Evaluation of a Novel Arg-Gly-Asp-conjugated α -melanocyte stimulating hormone hybrid peptide for potential melanoma therapy, *Bioconjug. Chem.* 20, 1634–1642.
- (18) C. Herold-Mende, H.H. Steiner, T. Andl, D. Riede, A. Buttler, C. Reisser, N.E. Fusenig and

- M.M. Mueller (1999) Expression and functional significance of vascular endothelial growth factor receptors in human tumor cells. *Lab Invest.* 12, 1573-1582.
- (19) N. Ferrara (2002) VEGF and the quest for tumour angiogenesis factors. *Nature Reviews Cancer* 2, 795-803.
- (20) M. Fani, D. Psimadas, C. Zikos, S. Xanthopoulos, G.K. Loudos, P. Bouziotis, A.D. Varvarigou (2006) Comparative evaluation of linear and cyclic ^{99m}Tc -RGD peptides for targeting of integrins in tumor angiogenesis. *Anticancer Res.* 26, 431–434.
- (21) N. Ferrara and T. Davis-Smyth (1997) The biology of vascular endothelial growth factor. *Endocr Rev.* 18, 4–25.
- (22) H. Abedi and I. Zachary (1997) Vascular Endothelial Growth Factor Stimulates Tyrosine Phosphorylation and Recruitment to New Focal Adhesions of Focal Adhesion Kinase and Paxillin in Endothelial Cells. *J Bio Chem.* 272, 15442-15451.
- (23) Y.A. Muller, B. Li, H.W. Christinger, J.A. Wells, B.C. Cunningham and A.M. de Vos (1997) Vascular endothelial growth factor: crystal structure and functional mapping of the kinase domain receptor binding site. *Proc Natl Acad Sci.* 94, 7192– 7197.
- (24) T. Asahara, T. Murohara, A. Sullivan, M. Silver, R. van der Zee, T. Li, B. Witzenbichler, G. Schatteman and J.M. Isner (1997) Isolation of putative progenitor endothelial cells for angiogenesis. *Science.* 275, 964–967.
- (25) J. Badet (1999) Angiogenin, a potent mediator of angiogenesis. Biological, biochemical and structural properties. Badet J, *Pathol Biol.* 47, 345-51.
- (26) B. P. Eliceiri and D. A. Cheresh (1999) The role of $\alpha_v\beta_3$ integrins during angiogenesis: insights into potential mechanisms of action and clinical development. *J Clin Invest.* 103, 1227–1230.

- (27) S. De, O. Razorenova, N.P. McCabe, T. O'Toole, J. Qin, and T. V. Byzova (2005) VEGF–integrin interplay controls tumor growth and vascularization. *Proc. Natl. Acad. Sci.*, 102, 7589–7594.
- (28) J.S. Desgrosellier and D.A. Cheresh (2010) Integrins in cancer: biological implications and therapeutic opportunities. *Nature Reviews Cancer* 10, 9-22.
- (29) H. Roland and C. Decristoforo (2009) Radiolabelled RGD peptides and peptidomimetics for tumour targeting. *Frontiers in Bioscience*. 14, 872-886.
- (30) Jay S. Desgrosellier and David A. Cheresh (2010) Integrins in cancer: biological implications and therapeutic opportunities, *Nat Rev Canc.* 10, 9-22.
- (31) W. Guo and F. G. Giancotti (2004) Integrin signalling during tumour progression. *Nature Reviews Molecular Cell Biology*. 5, 816-826.
- (32) D. L. Counter, L. Lomas, M. Scatena and C.M.Giachelli (2005) Src kinase activity is required for integrin $\alpha_v\beta_3$ - mediated activation of nuclear factor- κ B. *J. Biol. Chem.* 280, 12145–12151.
- (33) Y. Yamakita, G. Totsukawa, S. Yamashiro, D. Fry, X. Zhang, S. K. Hanks and F. Matsumura (1999) Dissociation of FAK/p130CAS/c-Src Complex during Mitosis: Role of Mitosis-specific Serine Phosphorylation of FAK. *JCB*. 144, 315-324.
- (34) K. Vuori, E. Ruoslahti (1994) Association of insulin receptor substrate-1 with integrins. *Science*. 266, 1576-1578.
- (35) S. Miyamoto, H. Teramoto, J.S. Gutkind, and K.M. Yamada (1996) Integrins can collaborate with growth factors for phosphorylation of receptor tyrosine kinases and MAP kinase activation: roles of integrin aggregation and occupancy of receptors. *JCB*. 135, 1633-1642.

- (36) A.S. Woodard, G. Garcia-Cardena, M. Leong, J.A. Madri, W.C. Sessa and L.R. Languino (1998) The synergistic activity of integrin $\alpha_v\beta_3$ and PDGF receptor increases cell migration. *J Cell Science*. 111, 469-478.
- (37) L. Moro, V. M. Bozzo, C. Bozzo, L. Silengo, F. Altruda, L. Beguinot, G. Tarone, P. Defilippi (1999) Integrins induce activation of EGF receptor: role in MAP kinase induction and adhesion-dependent cell survival. *EMBO Journal*. 17, 6622-6632.
- (38) R. Soldi, S. Mitola, M. Strasly, P. Defilippi, G. Tarone and F. Bussolino (1999) Role of $\alpha_v\beta_3$ integrin in the activation of vascular endothelial growth factor receptor-2. *EMBO Journal*. 18, 882-892.
- (39) R. Treisman (1996) Regulation of transcription by MAP kinase cascades. *Current Opinion in Cell Biology*. 8, 205-215.
- (40) K. R. Gehlsen, W. S. Argraves, M. D. Pierschbacher, and E. Ruoslahti (1988) Inhibition of in vitro tumor cells by Arg-Gly-Asp containing synthetic peptides. *JCB*. 106, 925-930.
- (41) R. Pytela, M. D. Pierschbacher and E. Ruoslahti (1985) A 125/115-kDa cell surface receptor specific for vitronectin interacts with the arginine-glycine-aspartic acid adhesion sequence derived from fibronectin. *Proc. Natl. Acad. Sci*. 82, 5766-5770.
- (42) E. Ruoslahti (1984) Fibronectin in cell adhesion and invasion. *Cancer Metastasis*. 3, 43-51.
- (43) M.D. Pierschbacher and E. Ruoslahti (1984) Variants of the cell recognition site of fibronectin that retain attachment-promoting activity. *Proc. Natl. Acad. Sci*. 81, 5985-5988.
- (44) M. J. Bissel and D. Radisky (2001) Putting tumors in context. *Nature Rev. Cancer* 1, 46-54.
- (45) B.S. Wiseman and Z. Werb (2002) Stromal effects on mammary gland development and

- breast cancer. *Science* 296, 1046–1049.
- (46) C. Müller-Tidow¹, S. Diederichs, E. Bulk, T. Pohle, B. Steffen, J. Schwäble, S. Plewka, M. Thomas, R. Metzger, P. M. Schneider, C. H. Brandts, W. E. Berdel and H. Serve (2005) Identification of Metastasis-Associated Receptor Tyrosine Kinases in Non-Small Cell Lung Cancer. *Cancer Research*. 65, 1778.
- (47) A. K. Perl, P. Wilgenbus, U. Dahl, H. Semb and G. Christofori (1998) A causal role for E-cadherin in the transition from adenoma to carcinoma. *Nature* 392, 190-193.
- (48) M.D. Sternlicht and Z. Werb (2001) How matrix metalloproteinases regulate cell behavior. *Annu. Rev. Cell Dev. Biol.* 17, 463–516.
- (49) S.M. Albelda et al. (1990) Integrin distribution in malignant melanoma: association of the β_3 subunit with tumor progression. *Cancer Res.* 50, 6757–6764.
- (50) C.L. Gladson and D.A. Cheresh (1991) Glioblastoma expression of vitronectin and the $\alpha_v\beta_3$ integrin: adhesion mechanism for transformed glial cells. *J. Clin. Invest.* 88, 1924–1932.
- (51) P.C. Brooks et al. (1996) Localization of matrix metalloproteinase MMP-2 to the surface of invasive cells by interaction with integrin $\alpha_v\beta_3$. *Cell* 85, 683–693.
- (52) F.G. Giancotti and G. Tarone (2003) Positional control of cell fate through joint integrin/receptor protein kinase signaling. *Annu. Rev. Cell Dev. Biol.* 19, 173–206.
- (53) C.K. Miranti and J.S. Brugge (2002) Sensing the environment: a historical perspective on integrin signal transduction. *Nature Cell Biol.* 4, 83–90.
- (54) S.M. Frisch and E. Ruoslahti (1997) Integrins and anoikis. *Curr. Opin. Cell Biol.* 9, 701–706.
- (55) A. Khwaja, P. Rodriguez-Viciana, S. Wennstrom, P.H. Warne and J. Downward (1997) Matrix adhesion and Ras transformation both activate a phosphoinositide 3-OH kinase and

- protein kinase B/Akt cellular survival pathway. *EMBO J.* 16, 2783–2793.
- (56) M.J. Reginato et al. (2003) Integrins and EGFR coordinately regulate the pro-apoptotic protein Bim to prevent anoikis. *Nature Cell Biol.* 5, 733–740.
- (57) J. S. Fridman and S.W. Lowe (2003) Control of apoptosis by p53. *Oncogene* 22, 9030–9040.
- (58) J.P. Thiery (2002) Epithelial–mesenchymal transitions in tumour progression. *Nature Rev. Cancer.* 2, 442–454.
- (59) K. Alitalo and P. Carmeliet (2002) Molecular mechanisms of lymphangiogenesis in health and disease. *Cancer Cell.* 1, 219–227.
- (60) B. Felding-Habermann et al. (2001) Integrin activation controls metastasis in human breast cancer. *Proc. Natl Acad. Sci.* 98, 1853–1858.
- (61) L. Borsig, R. Wong, R.O. Hynes, N.M. Varki, and A. Varki (2002) Synergistic effects of L- and P-selectin in facilitating tumor metastasis can involve non-mucin ligands and implicate leukocytes as enhancers of metastasis. *Proc. Natl Acad. Sci.* 99, 2193–2198.
- (62) L.M. Coussens and Z. Werb (2002) Inflammation and cancer. *Nature* 420, 860–867.
- (63) R. Haubner, R. Gratias, B. Diefenbach, S. Goodman, A. Jonczyk and H. Kessler (1996) Structural and functional aspects of RGD-containing cyclic pentapeptides as highly potent and selective integrin $\alpha_v\beta_3$ antagonists. *J Am Chem Soc.* 118, 7461–72.
- (64) R. Haubner, H-J. Wester, F. Burkhart, R. Senekowitsch-Schmidtke, W. Weber, S. Goodman et al. (2001) Glycosylated RGD-containing peptides: tracer for tumor targeting and angiogenesis imaging with improved biokinetics. *J Nucl Med.* 42, 326–36.
- (65) M.A. Schwartz, M.D. Schaller and M.H. Ginsberg (1995) *Annu. Rev. Cell. Dev. Biol.* 11, 549–599.

- (66) P.C. Brooks, R.A. Clark, D.A. Cheresh (1994) Requirements of vascular integrin $\alpha_v\beta_3$ for angiogenesis. *Science*. 264, 569-571.
- (67) M.S. Albelda, S.A. Mette, D.E. Elder, R. Stewart, L. Damjanovich, M. Herlyn and Clayton A. Buck (1990) Integrin Distribution in Malignant Melanoma: Association of the β_3 Subunit with Tumor Progression. *Cancer Res.* 50, 6757-6764.
- (68) M. Zhao, Y. Gao, L. Wang, S. Liu, B. Han, L. Ma, Y. Ling, S. Mao and X. Wang (2013) Overexpression of integrin-linked kinase promotes lung cancer cell migration and invasion via NF- κ B-mediated upregulation of matrix metalloproteinase-9. *Int J Med Sci.* 10, 995-1002
- (69) I. Dijkgraaf, J.A. Kruijtzter, C. Frielink, A.C. Soede, H.W. Hilbers, W.J. Oyen, F.H. Corstens, R.M. Liskamp, O.C. Boerman (2006) Synthesis and biological evaluation of potent $\alpha_v\beta_3$ -integrin receptor antagonists. *Nucl. Med. Biol.* 33, 953–961.
- (70) D.G. Stupack, X.S. Puente, S. Boutsaboualoy, C.M. Storgard, D.A. Cheresh (2001) Apoptosis of adherent cells by recruitment of caspase-8 to unligated integrins. *Cell Biol.* 155, 459-470.
- (71) F. Aoudjit, and K. Vuori (2001) Matrix attachment regulates Fas-induced apoptosis in endothelial cells: a role for c-flip and implications for anoikis. *J Cell Biol.* 152, 633–643.
- (72) F. Aoudjit and K. Vuori (2001) Integrin signaling inhibits paclitaxel-induced apoptosis in breast cancer cells. *Oncogene* 20, 4995–5004.
- (73) M. Scaten et al. (1998) NF- κ B mediates $\alpha_v\beta_3$ integrin- induced endothelial cell survival. *J. Cell Biol.* 141, 1083–1093.
- (74) W. Bao and S. Stromblad (2004) Integrin α_v -mediated inactivation of p53 controls a MEK1-dependent melanoma cell survival pathway in three-dimensional collagen. *J. Cell*

- Biol.* 167, 745–756.
- (75) D.G. Stupack, X.S. Puente, S. Boutsaboualoy, C.M. Storgard and D.A. Cheresh (2001) Apoptosis of adherent cells by recruitment of caspase-8 to unligated integrins. *J. Cell Biol.* 155, 459–470.
- (76) D.G. Stupack et al. (2006) Potentiation of neuroblastoma metastasis by loss of caspase-8. *Nature* 439, 95–99.
- (77) S.J. Bakewell et al. (2003) Platelet and osteoclast β_3 integrins are critical for bone metastasis. *Proc. Natl Acad. Sci.* 100, 14205–14210.
- (78) S. Liu (2008) Bifunctional coupling agents for target-specific delivery of metallic radionuclides. *Adv. Drug Delivery Rev.* 60, 1347–1370.
- (79) D.A. Mankoff, J.M. Link, H.M. Linden, L. Sundararajan, K.A. Krohn (2008) Tumor receptor imaging. *J Nucl Med.* 49, 149-163.
- (80) W.H. Miller, R.M. Keenan, R.N. Willette, M.W. Lark (2000) Identification and in vivo efficacy of small-molecule antagonists of integrin $\alpha_v\beta_3$ (the vitronectin receptor). *DDT(Drug Discovery Today)*. 5, 397-408.
- (81) J.C. Reubi, H.R. Macke and E.P. Krenning (2005) Candidates for peptide receptor radiotherapy today and in the future. *J. Nucl. Med.* 46, 67–75.
- (82) Z. Liu, F. Wang and X. Chen (2008) Integrin $\alpha_v\beta_3$ -Targeted Cancer Therapy. *Drug Dev Res.* 69, 329–339.
- (83) S. Liu (2006) Radiolabeled Multimeric Cyclic RGD Peptides as Integrin $\alpha_v\beta_3$ Targeted Radiotracers for Tumor Imaging. *Molecular Pharmaceutics.* 3, 474-487.
- (84) P.C. Brooks, R.A. Clark and D.A. Cheresh (1994) Requirement of vascular integrin $\alpha_v\beta_3$ for angiogenesis. *Science.* 264, 569–571.

- (85) M. Friedlander, P.C. Brooks, R.W. Shaffer, C.M. Kincaid, J.A. Varner, D.A. Cheresh (1995) Definition of two angiogenic pathways by distinct α_v integrins. *Science*. 270, 1500–1502.
- (86) C.C. Kumar (2003) Integrin $\alpha_v\beta_3$ as a therapeutic target for blocking tumor-induced angiogenesis. *Curr Drug Targets*. 4, 123–131.
- (87) A.J. Beer, R. Haubner, I. Wolf et al. (2006) PET-based human dosimetry of ^{18}F -galacto-RGD, a new radiotracer for imaging $\alpha_v\beta_3$ expression. *J Nucl Med*. 47, 763–769.
- (88) D. Meitar, S.E. Crawford, A.W. Rademaker, S.L. Cohn (1996) Tumor angiogenesis correlates with metastatic disease, N-myc amplification, and poor outcome in human neuroblastoma. *J Clin Oncol*. 14, 405–414.
- (89) K. Meerovitch, F. Bergeron, L. Leblond, B. Grouix, C. Poirier, M. Bubenik, L. Chan, H. Gourdeau, T. Bowlin, G. Attardo (2003) A novel RGD antagonist that targets both $\alpha_v\beta_3$ and $\alpha_5\beta_1$ induces apoptosis of angiogenic endothelial cells on type I collagen. *Vascul Pharmacol*. 40, 77-89.
- (90) P.A. Burke, S.J. DeNardo (2001) Antiangiogenic agents and their promising potential in combined therapy. *Crit. Rev. Oncol. Hematol*. 39, 155-171.
- (91) R.L. Qiao, W.H. Yan, H. Lum, A. B. Malik (1995) Arg-Gly-Asp peptide increases endothelial hydraulic conductivity: comparison with thrombin response. *Am. J. Physiol*. 269, 110-117.
- (92) I. Buchmann, M. Henze, S. Engelbrecht, M. Eisenhut, A. Runz, M. Schafer, T. Schilling, S. Haufe, T. Herrmann, U. Haberkorn (2007) Comparison of ^{68}Ga -DOTATOC PET and ^{111}In -DTPAOC (Octreoscan) SPECT in patients with neuroendocrine tumours. *Eur. J. Nucl. Med. and Mol. Imaging*. 34, 1617–1626.
- (93) M. Fani, J.P. Andre, H.R. Maecke (2008) ^{68}Ga -PET: A powerful generator-based alternative

- to cyclotron-based PET radiopharmaceuticals. *Contrast Media Mol. Imaging.* 3, 67–77.
- (94) J.C. Reubi, H.R. Macke, E.P. Krenning (2005) Candidates for peptide receptor radiotherapy today and in the future. *J. Nucl. Med.* 46, 67–75.
- (95) K. Tanaka, K. Fukase (2008) PET (positron emission tomography) imaging of biomolecules using metal-DOTA complexes: A new collaborative challenge by chemists, biologists, and physicians for future diagnostics and exploration of in vivo dynamics. *Org. Biomol. Chem.* 6, 815–828.
- (96) J. Notni, K. Pohle, H.J. Wester (2012) Comparative gallium-68 labeling of TRAP-, NOTA-, and DOTA-peptides: Practical consequences for the future of gallium-68-PET. *EJNMMI Res.* 2, 28-33.
- (97) K. Chen, J. Xie, and X. Chen (2009) RGD-Human Serum Albumin Conjugates as Efficient Tumor Targeting Probes. *Molecular Imaging.* 8, 65-73.
- (98) B. Guerin, S. Ait-Mohand, M.C. Tremblay, V. Dumulon-Perreault, P. Fournier, F. Benard, (2010) Total solid-phase synthesis of NOTA-functionalized peptides for PET imaging. *Org. Lett.* 12, 280–283.
- (99) T. Poethko, M. Schottelius, G. Thumshirn, M. Herz, R. Haubner, G. Henriksen, H. Kessler, M. Schwaiger and H.J. Wester (2004) Chemoselective pre-conjugate radiohalogenation of unprotected mono- and multimeric peptides via oxime formation. *Radiochim. Acta* 92, 317–327.
- (100) T. Poethko, M. Schottelius, G. Thumshirn, U. Hersel, M. Herz, G. Henriksen, H. Kessler, M. Schwaige and H.J. Wester (2004) Two-step methodology for high yield routine radiohalogenation of peptides: ¹⁸F-labeled RGD and octreotide analogs. *J. Nucl. Med.* 45, 892–902.

- (101) D. Boturyn, J.L. Coll, E. Garanger, M.C. Favrot and P. Dumy (2004) Template assembled cyclopeptides as multimeric system for integrin targeting and endocytosis. *J. Am. Chem. Soc.* 126, 5730–5739.
- (102) Y. Wu, X. Zhang, Z. Xiong, Z. Cheng, D.R. Fisher, S. Liu, S.S. Gambhir and X. Chen (2005) MicroPET imaging of glioma integrin $\alpha_v\beta_3$ expression using ^{64}Cu -labeled tetrameric RGD peptide. *J. Nucl. Med.* 46, 1707–1718.
- (103) M. Janssen, W. J. G. Oyen, L. F. A. G. Massuger, C. Frielink, I. Dijkgraaf, D. S. Edwards, M. Rajopadhye, F. H. M. Corsten and O. C. Boerman (2002) Comparison of a monomeric and dimeric radiolabeled RGD-peptide for tumor targeting. *Cancer Biotherapy & Radiopharmaceuticals.* 17, 641-646.
- (104) S. Liu (2009) Radiolabeled cyclic RGD peptides as integrin $\alpha_v\beta_3$ -targeted radiotracers: maximizing binding affinity via bivalency. *Bioconj Chem.* 20, 2199-213.
- (105) B. S. Wiseman and Z. Werb (2002) Stromal elects of mammary gland development and breast cancer. *Science.* 296, 1046-1049.
- (106) S. Ji, A. Czerwinski, Y. Zhou, G. Shao, F. Valenzuela, P. Sowiński, S. Chauhan, M. Pennington, and S. Liu (2013) $^{99\text{m}}\text{Tc}$ -Galacto-RGD2: a $^{99\text{m}}\text{Tc}$ -labeled cyclic RGD peptide dimer useful for tumor imaging. *Mol. Pharm. In press.* 10, 3304–3314
- (107) J. Shi, Y. Zhou, S. Chakraborty, Y.-S. Kim, B. Jia, F. Wang and S. Liu (2011) Evaluation of ^{111}In -Labeled Cyclic RGD Peptides: Effects of Peptide and Linker Multiplicity on Their Tumor Uptake, Excretion Kinetics and Metabolic Stability. *Theranostics.* 1, 322-340.
- (108) P. C. Brooks, A. M. P. Montgomery, M. Rosenfeld, R. Reisfeld, T. H. Hu, G. Klier, D. A. Cheresh (1994) Integrin $\alpha_v\beta_3$ antagonists promote tumor regression by inducing apoptosis of angiogenic blood vessels. *Cell.* 79, 1157-1164.

- (109) A. Giannis, F. Rubsam C(1997) Integrin antagonists and other low molecular weight compounds as inhibitors of angiogenesis: new drugs in cancer therapy. *Angew. Chem.Int.Ed. Engl.* 36, 588- 590.
- (110) C. P. Carron, D. M. Meyer, V. W. Engleman, J. G. Rico, P. G. Ruminiski, R.L. Ornberg, W. F. Westlin, G. A. Nickols (2000) Peptidomimetic antagonists of $\alpha_v\beta_3$ inhibit bone resorption by inhibiting osteoclast bone resorptive activity, not osteoclast adhesion to bone. *J Endocrinol.* 165, 587-98.
- (111) M. Piert, H.J. Machulla, M. Picchio, G. Reischl, S. Ziegler, P. Kumar et al. (2005) Hypoxia-Specific Tumor Imaging with ^{18}F -Fluoroazomycin Arabinoside. *J Nucl Med.* 46, 106-13.
- (112) B. E. Rogers, H. M. Bigott, D. W. McCarthy, D. Della Manna, J. Kim, T. L. Sharp, M. J. Welch (2003) MicroPET imaging of a gastrin-releasing peptide receptor-positive tumor in a mouse model of human prostate cancer using a ^{64}Cu -labeled bombesin analogue. *Bioconjug Chem.* 14, 756-63.
- (113) J. C. Miller, H. H. Pien, D. Sahani, A. G. Sorensen, J. H. Thrall (2005) Imaging angiogenesis: applications and potential for drug development. *J Natl Cancer Inst.* 2, 172-87.
- (114) F. G. Giancotti and G. Tarone (2003) Positional control of cell fate through joint integrin/receptor protein kinase signaling. *Annu. Rev. Cell Dev. Biol.* 19, 173–206.
- (115) F. G. Blankenberg, S. Mandl, Y. A. Cao, C. O'Connell-Rodwell, C. Contag, C. Mari et al. (2004) Tumor imaging using a standardized radiolabeled adapter protein docked to vascular endothelial growth factor. *J Nucl Med.* 45, 1373-80.
- (116) C. K. Miranti and J. S. Brugge (2002) Sensing the environment: a historical perspective on integrin signal transduction. *Nature Cell Biol.* 4, 83–90.

- (117) J. C. Miller, H. H. Pien, D. Sahani, A. G. Sorensen, J. H. Thrall (2005) Imaging Angiogenesis: Applications and Potential for Drug Development. *J Natl Cancer Inst.* 97, 172-187.
- (118) M. N. Wernick, J. N. Aarsvold (2004) Emission Tomography: The Fundamentals of SPECT and PET, 1st ed, Elsevier, San Diego, CA.
- (119) Gopal B. Saha (1997) Fundamentals of Nuclear Pharmacy, Springer, 1997 Fourth Edition.
- (120) C. M. Gomesa, A. J. Abrunhosab, P. Ramosc, E. K. J. Pauwelsd. (2011) Molecular imaging with SPECT as a tool for drug development. *Advanced Drug delivery system.* 63, 547-554.
- (121) M. T. Madsen (2007) Recent advances in SPECT imaging. *J. Nucl. Med.* 48, 661-673.
- (122) S. M. Okarvi (2004) Peptide-based radiopharmaceuticals: future tools for diagnostic imaging of cancers and other diseases. *Med Res Rev.* 2004; 24, 357-97.
- (123) P. Antunes, M. Ginj, M.A. Walter, J. Chen, J. C. Reubi, H. R. Maecke (2007) Influence of different spacers on the biological profile of a DOTA-somatostatin analogue. *Bioconjug Chem.* 18, 84-92.
- (124) M. Fani, H. R. Maecke¹, S. M. Okarvi (2012) Radiolabeled Peptides: Valuable Tools for the Detection and Treatment of Cancer. *Theranostics.* 2, 481-501.
- (125) R. Haubner, H. J. Wester, U. Reuning, R. Senekowitsch-Schmidtke, B. Diefenbach, H. Kessler et al. (1999) Radiolabeled $\alpha_v\beta_3$ integrin antagonists: a new class of tracers for tumor targeting. *J.Nucl Med.* 40, 1061-71.
- (126) A. J. Beer, R. Haubner, I. Wolf, M. Goebel, S. Luderschmidt, M. Niemeyer et al. (2006) PET-based human dosimetry of ^{18}F -galacto-RGD, a new radiotracer for imaging $\alpha_v\beta_3$ expression. *J Nucl Med.* 47, 763-9.
- (127) A. J. Beer, R. Haubner, M. Sarbia, M. Goebel, S. Luderschmidt, A.L. Grosu et al. (2006)

- Positron emission tomography using [^{18}F] Galacto-RGD identifies the level of integrin $\alpha_v\beta_3$ expression in man. *Clin Cancer Res.* 12, 3942–9.
- (128) W. Cai, J. Rao, S. S. Gambhir, X. Chen (2006) How molecular imaging is speeding up antiangiogenic drug development. *Mol. Cancer Ther.* 5, 2624–2633.
- (129) A. J. Beer, R. Haubner, M. Goebel, S. Luderschmidt, M. E. Spilker, H. J. Wester et al. (2005) Biodistribution and pharmacokinetics of the $\alpha_v\beta_3$ -selective tracer ^{18}F -galacto-RGD in cancer patients. *J Nucl Med* 2005. 46, 1333–41.
- (130) Liu, S., Hsieh, W. Y., Jiang, Y., Kim, Y. S., Sreerama, S. G., Chen, X., Jia, B., Wang, F. (2007) Evaluation of a $^{99\text{m}}\text{Tc}$ -labeled cyclic RGD tetramer for noninvasive imaging $\alpha_v\beta_3$ integrin-positive breast cancer. *Bioconjugate Chem.* 18, 438-446.
- (131) Wang, L., Shi, J., Kim, Y. S., Zhai, S., Jia, B., Zhao, H., Liu, Z., Wang, F., Chen, X., Liu, S. (2009) Improving tumor targeting capability and pharmacokinetics of $^{99\text{m}}\text{Tc}$ -labeled cyclic RGD dimers with PEG₄ linkers. *Mol. Pharm.* 6, 231-245.
- (132) Shi, J., Wang, L., Kim, Y. S., Zhai, S., Liu, Z., Chen, X., Liu, S. (2008) Improving tumor uptake and excretion kinetics of $^{99\text{m}}\text{Tc}$ -labeled cyclic Arginine-Glycine-Aspartic (RGD) dimers with triglycine linkers. *J. Med. Chem.* 51, 7980-7990.
- (133) Shi, J., Wang, L., Kim, Y. S., Zhai, S., Jia, B., Wang, F., Liu, S. (2009) $^{99\text{m}}\text{TcO}(\text{MAG}_2\text{-}3\text{G}_3\text{-dimer})$: A new integrin $\alpha_v\beta_3$ -targeted radiotracer with high tumor uptake and favorable pharmacokinetics. *Eur. J. Nucl. Med. Mol. Imaging* 36, 1874-1884.
- (134) Shi, J., Kim, Y. S., Zhai, S., Liu, Z., Chen, X., Liu, S. (2009) Improving tumor uptake and pharmacokinetics of ^{64}Cu -labeled cyclic RGD dimers with triglycine and PEG₄ linkers. *Bioconjugate Chem.* 20, 750-759.
- (135) Shi, J., Kim, Y. S., Chakraborty, S., Jia, B., Wang, F., Liu, S. (2009) 2-

- Mercaptoacetylglycylglycyl (MAG₂) as a bifunctional chelator for ^{99m}Tc-labeling of cyclic RGD dimers: effects of technetium chelate on tumor uptake and pharmacokinetics. *Bioconjugate Chem.* 20, 1559-1568.
- (136) Chakraborty, S., Shi, J., Kim, Y. S., Zhou, Y., Jia B., Wang, F., Liu, S. (2010) Evaluation of ¹¹¹In-labeled cyclic RGD peptides: tetrameric not tetravalent. *Bioconjugate Chem.* 21, 969-978.
- (137) Zhou, Y., Kim, Y. S., Chakraborty, S., Shi, J., Gao, H., Liu, S. (2011) ^{99m}Tc-Labeled cyclic RGD peptides for noninvasive monitoring of tumor integrin $\alpha_v\beta_3$ expression. *Mol. Imaging* 10, 386-97.
- (138) Shi, J., Zhou, Y., Chakraborty, S., Kim, Y. S., Jia, B., Wang, F., Liu, S. (2011) Evaluation of ¹¹¹In-labeled cyclic RGD peptides: effects of peptide and PEG₄ multiplicity on their tumor uptake, excretion kinetics and metabolic stability. *Theranostics* 1, 322-340.
- (139) Shi, J., Kim, Y. S., Chakraborty, S., Zhou, Y., Wang, F., and Liu, S. (2011) Impact of bifunctional chelators on biological properties of ¹¹¹In-labeled cyclic peptide RGD dimers. *Amino Acids* 41, 1059-1070.
- (140) Zhou, Y., Kim, Y. S., Lu, X., Liu, S. (2012) Evaluation of ^{99m}Tc-labeled cyclic RGD dimers: impact of cyclic RGD peptides and ^{99m}Tc chelates on biological properties. *Bioconjugate Chem.* 23, 586–595.
- (141) Zhou, Y., Kim, Y. S., Chakraborty, S., Shi, J., Gao, H., and Liu, S. (2011) ^{99m}Tc-labeled cyclic RGD peptides for noninvasive monitoring of tumor integrin $\alpha_v\beta_3$ expression. *Mol. Imaging* 10, 386-397.
- (142) Ji, S., Czerwinski, A., Zhou, Y., Shao, G., Valenzuela, F., Sowiński, P., Chauhan, S., Pennington, M., and Liu, S. (2013) ^{99m}Tc-Galacto-RGD₂: a ^{99m}Tc-labeled cyclic RGD

- peptide dimer useful for tumor imaging. *Mol. Pharm. In press.*
- (143) Dijkgraaf, I., Kruijtzter, J. A., Liu, S., Soede, A. C., Oyen, W. J., Corstens, F. H., Liskamp, R. M., Boerman, O. C. (2007) Improved targeting of the $\alpha_v\beta_3$ integrin by multimerization of RGD peptides. *Eur. J. Nucl. Med. Mol. Imaging* 34, 267-273.
- (144) Haubner, R., Beer, A. J., Wang, H., and Chen, X. (2010) Positron emission tomography tracers for imaging angiogenesis. *Eur. J. Nucl. Med. Mol. Imaging* 37 (Suppl. 1), S86-103.
- (145) Ji, S., Czerwinski, A., Zhou, Y., Shao, G., Valenzuela, F., Sowiński, P., Chauhan, S., Pennington, M., and Liu, S. (2013) ^{99m}Tc -Galacto-RGD₂: a ^{99m}Tc -labeled cyclic RGD peptide dimer useful for tumor imaging. *Mol. Pharm. In press.*
- (146) Onthank, D.C., Liu, S., Silva, P.J., Barrett, J.A., Harris, T.D., Robinson, S.P., and Edwards, D.S. (2004) ^{90}Y and ^{111}In complexes of A DOTA-conjugated integrin $\alpha_v\beta_3$ receptor antagonist: different but biologically equivalent. *Bioconjugate Chem.* 15, 235-41.
- (147) Cremonesi, M., Ferrari, M., Zoboli, S., Chinol, M., Stabin, M. G., Orsi, F., Maecke, H. R., Jermann, E., Robertson, C., Fiorenza, M., Tosi, G., and Paganelli, G. (1999) Biokinetics and dosimetry in patients administered with ^{111}In -DOTA-Tyr³-octreotide: implications for internal radiotherapy with ^{90}Y -DOTATOC. *Eur. J. Nucl. Med.*, 26, 877-886.
- (148) De Jong, M., Bakker, W. H., Krenning, E. P., Breeman, W. A. P., van der Pluijm, M. E., Bernard, B., Visser, T. J., Jermann, E., Béhé, M., Powell, P., and Mäcke, H. (1997) Yttrium-90 and indium-111 labeling, receptor binding and biodistribution of [DOTA⁰,-D-Phe¹, Tyr³]octreotide, a promising somatostatin analogue for radionuclide therapy. *Eur. J. Nucl. Med.* 24, 368-371.
- (149) De Jong, M., Bakker, W. H., Bernard, B. F., Valkema, R., Kwekkeboom, D. J., Reubi, J. C., Srinivasan, A., Schmidt, M., and Krenning, E. P. (1999) Preclinical and initial clinical

- evaluation of ^{111}In -labeled nonsulfated CCK₈ analog: a peptide for CCK-B receptor targeted scintigraphy and radionuclide therapy. *J. Nucl. Med.* 40, 2081-2087.
- (150) Aloj, L., Cacraco, C., Panico, M., Zannetti, A., Del Vecchio, S., Tesauero, D., De Luca, S., Arra, C., Pedone, C., Morelli, G., and Salvatore, M. (2004) In-vitro and in-vivo evaluation of ^{111}In -DTPAGlu-G-CCK8 for cholestykinin-B-receptor imaging. *J. Nucl. Med.* 45, 485-494.
- (151) De Visser, M., Bernard, H. F., Erion, J. L., Schmidt, M. A., Srinivasan, A., Waser, B., Reubi, J. C., Krenning, E. P., and de Jong, M. (2007) Novel ^{111}In -labelled bombesin analogues for molecular imaging of prostate tumors. *Eur. J. Nucl. Med. Mol. Imaging* 34, 1228-1238.
- (152) Heppeler, A., Froidevaux, S., Mäcke, H. R., Jermann, E., Béhé, M., Powell, P., and Hennig, M. (1999) Radiometal-labelled macrocyclic chelator-derivatised somatostatin analogue with superb tumour targeting properties and potential for receptor-mediated internal radiotherapy. *Chem. Eur. J.* 5, 1974-1981.
- (153) Kwekkeboom, D. J., de Herder, W. W., Kam, B. L., van Eijck, C. K., van Essen, M., Kooij, P.P., Feelders, R. A., van Aken, M. O., and Krenning, E. P. (2008) Treatment with the radiolabeled somatostatin analog [^{177}Lu -DOTA⁰,Tyr³]octreotate: toxicity, efficacy and survival. *J. Clin. Oncol.* 26, 2114-2130.
- (154) Harris, T.D., Kalogeropoulos, S., Nguyen, T., Dwyer, G., Edwards, D.S., Liu, S., Bartis, J., Ellars, C., Onthank, D., Yalamanchili, P., Heminway, S., Robinson, S., Lazewatsky, J., and Barrett, J. (2006) Structure-Activity relationships of ^{111}In - and $^{99\text{m}}\text{Tc}$ -labeled quinolin-4-one peptidomimetics as ligands for the vitronectin receptor: potential tumor imaging agents. *Bioconjugate Chem.*, 17, 1294-1313.
- (155) Wagh, N. K., Zhou, Z., Ogbomo, S. M., Shi, W., and Brusnahan, S. K. (2012) Garrison JC.

- Development of hypoxia enhanced ^{111}In -labeled bombesin conjugates: design, synthesis, and in vitro evaluation in PC-3 human prostate cancer. *Bioconjugate Chem.* 2012 Feb 16.
- (156) Liu, S. (2008) Bifunctional coupling agents for radiolabeling of biomolecules and target-specific delivery of metallic radionuclides. *Adv. Drug Delivery Rev.* 60, 1347-1370.
- (157) Fani, M., and Maecke, H. (2012) Radiopharmaceutical development of radiolabelled peptides. *Eur. J. Nucl. Med. Mol. Imaging* 39,11-30.
- (158) Haubner, R., Wester, H. J. (2004) Radiolabeled tracers for imaging of tumor angiogenesis and evaluation of anti-angiogenic therapies. *Curr. Pharm. Des.* 10, 1439-1455.
- (159) Liu, S. (2006) Radiolabeled multimeric cyclic RGD peptides as $\alpha_v\beta_3$ integrin-targeted radiotracers for tumor imaging. *Mol. Pharm.* 3, 472-487.
- (160) Liu, S. (2009) Radiolabeled RGD peptides as integrin $\alpha_v\beta_3$ -targeted radiotracers: maximizing binding affinity via bivalency. *Bioconjugate Chem.* 20, 2199-2213.
- (161) Suzuki, M., Mose, E. S., Montel, V., Tarin, D. (2006) Dormant cancer cells retrieved from metastasis-free organs regain tumorigenic and metastatic potency. *Am. J. Pathol.* 169, 673-681.
- (162) Sellappan, S., Grijalva, R., Zhou, X., Yang, W., Eli, M. B., Mills, G. B., Yu, D. (2004) Lineage infidelity of MDA-MB-435 cells: expression of melanocyte proteins in a breast cancer cell line. *Cancer Res.* 64, 3479-3485.
- (163) Ellison, G., Klinowska, T., Westwood, R. F., Docter, E., French, T., Fox, J. C. (2002) Further evidence to support the melanocytic origin of MDA-MB-435. *Mol. Pathol.* 55, 294-299.
- (164) Chambers, A. F. (2009) MDA-MB-435 and M14 cell lines: identical but not M14 melanoma. *Cancer Res.* 69, 5292-5293.

- (165) Haubner, R., Wester, H. J., Weber, W. A., Mang, C., Ziegler, S. I., Goodman, S. L., Senekowitsch-Schmidtke, R., Kessler, H., Schwaiger, M. (2001) Noninvasive imaging of $\alpha_v\beta_3$ integrin expression using ^{18}F -labeled RGD-containing glycopeptide and positron emission tomography. *Cancer Res.* 61, 1781-1785.
- (166) Haubner, R., Wester, H. J., Burkhart, F., Senekowitsch-Schmidtke, R., Weber, W., Goodman, S. L., Kessler, H., Schwaiger, M. (2001) Glycosylated RGD-containing peptides: tracer for tumor targeting and angiogenesis imaging with improved biokinetics. *J. Nucl. Med.* 42, 326-336.
- (167) Haubner, R., Kuhnast, B., Mang, C., Weber, W. A., Kessler, H., Wester, H. J., Schwaiger, M. (2004) [^{18}F]Galacto-RGD: synthesis, metabolic Stability, and radiation dose estimates. *Bioconjugate Chem.* 15, 61-69.
- (168) Doss, M., Kolb, H.C., Zhang, J.J., Bélanger, M.J., Stubbs, J.B., Stabin, M.G., Hostetler, E.D., Alpaugh, R.K., Mehren, M., Walsh, J.C., Haka, M., Mocharla, V.P., Yu, J.Q. (2012) Biodistribution and radiation dosimetry of the integrin marker ^{18}F -RGD-K₅ determined from whole-body PET/CT in monkeys and humans. *J. Nucl. Med.* 53, 787-795.
- (169) Morais, G. R., Falconer, R. A., and Santos, I. (2013) Carbohydrate-based molecules for molecular imaging in nuclear medicine. *Eur. J. Org. Chem.* 1401–1414.
- (170) B. Jia , J. Shi , Z. Yang , B. Xu , Z. Liu , H. Zhao , S. Liu and F. Wang (2006) $^{99\text{m}}\text{Tc}$ -Labeled Cyclic RGDfK Dimer: Initial Evaluation for SPECT Imaging of Glioma. *Bioconjugate Chem.* 17, 1069–1076.
- (171) C. Decristoforo, B. Faintuch-Linkowskib, A. Reyc, E. von Guggenberg, M. Rupprich, I. Hernandez-Gonzales, T. Rodrigo, R. Haubner (2006) [$^{99\text{m}}\text{Tc}$]HYNIC-RGD for imaging integrin $\alpha_v\beta_3$ expression. *Nuclear Medicine and Biology.* 33, 945–952.

- (172) J.M. Jeong, Y.J. Kim, Y.S. Lee, D.S. Lee, J.K. Chung, M.C. Lee (2009) Radiolabeling of NOTA and DOTA with Positron Emitting ^{68}Ga and Investigation of In Vitro Properties. *Nucl Med Molec Imaging*. 43, 330-336.
- (173) C.J. Broan, JPL Cox, AS. Craig, R. Katakya, D. Parker, A. Harrison, AM. Randall, G. Ferguson (1991) Structure and solution stability of indium and gallium complexes of 1,4,7-triazacyclononanetriacetate and of yttrium complexes of 1,4,7,10-tetraazacyclododecanetetraacetate and related ligands: kinetically stable complexes for use in imaging and radioimmunotherapy. X-ray molecular structure of the indium and gallium complexes of 1,4,7-triazacyclononane-1,4,7-triacetic acid. *J Chem Soc Perkin Trans*. 21, 87–99.
- (174) AS. Craig, D. Parker, H. Adams, NA. Bailey. (1989) Stability, gallium-71 NMR and crystal structure of a neutral gallium(III) complex of 1,4,7- triazacyclononanetriacetate: a potential radiopharmaceutical? *J Chem Soc Chem Commun*. 23, 1793–1794.
- (175) A. Heppeler, S. Froidevaux, HR. Mäcke, E. Jermann, M. Béhé, P. Powell, M. Hennig (1999) Radiometal-labelled macrocyclic chelator-derivatized somatostatin analogue with superb tumour-targeting properties and potential for receptor-mediated internal radiotherapy. *Chem Eur J*. 5, 1974–1981.

7. List of abbreviations

SRC	Proto-Oncogene Tyrosine Kinase
RAS	Rat Sarcoma
HIF-1	Hypoxia Inducible Factor 1
HRE	Hypoxia Response Factor
VEGF	Vascular Endothelial Growth factor
CAIX	Carbonic Anhydrase IX
PDGF	Platelet Derived Growth Factor
TGF-α	Transforming Growth Factor- α
FH-1	Fumarate Hydratase-1
KDR	Kinase Insert Domain Receptor
FLK-1	Tyrosine Kinase Receptor for VEGF
bFGF	Basic Fibroblast Factor
ECM	extracellular matrix
FAK	focal adhesion kinase
ILK	integrin-linked kinase
MAPK	mitogen activated protein kinase
ERK	extracellular-signal-regulated-kinase
EGF	epidermal growth factor
TCF	ternary complex factor
RDG	Arginin-Glycine-Aspartic Acid sequence
IMD	integrin mediated death
TGF-β	transforming growth factor- β

FGF2	fibroblast growth factor 2
uPA	urokinase plasminogen activator
RTK	Receptor Tyrosine Kinase
CT	Computed Tomography
MRI	Magnetic Resonance Imaging
PET	Positron Emission Tomatography
SPECT	Single Photon Emission Chromatography
FDG	Fluorodesoxyglucose
BM	Biomolecule
BFC	Biofunctional chelator
DTPA	Diethylenetriaminepentaacetic acid
DOTA	1,4,7,10-tetraazacyclododecane-1,4,7,10-tetraacetic acid
NOTA	1,4,7-triazacyclononane-N,N',N"-triacetic acid
NODASA	NOTA with aspartic acid
NODAGA	NOTA with glutamic acid
NODAPA-NCS	NOTA with benzyl-isothiocyanate
SAA	7-amino-L-glycero-L-galacto-2,6-anhydro-7-deoxyheptanamide
PEG2	6-dioxaoctanoic acid
HYNIC	6-hydrazinonicotinyl
NOTA-bz	2-(p-thioureidobenzyl)-1,4,7-triazacyclononane-1,4,7-triacetic acid
3P-RGD	PEG4-E[PEG4-c(RGDfK)]2
PEG4	PEG4 = 15-amino-4,7,10,13-tetraoxapentadecanoic acid
DOTA-OSu	1,4,7,10-tetraazacyclododecane-4,7,10-triaceticacid-1-acetate(N-

	hydroxysuccinimide)
SCN-Bz-NOTA	2-(p-thiocyanatobenzyl)-1,4,7-triazacyclononane-1,4,7-triacetic acid
MALDI	matrix assisted laser desorption ionizations
DMF	dimethylformamide
DIEA	diisopropylethylamine
IC50	half maximal inhibitory concentration
FITC	fluorescein isothiocyanate
EDTA	Ethylenediaminetetraacetic acid
%ID/gr	% Injected Dose per Gram Tissue (Unit used for Biodistribution)

8. Curriculum Vitae

Name: Elena Tomaselli

Date of birth: 26.09.1990

Place of birth: Trento, Italy

Parents: Claudia e Fiorenzo Tomaselli

Address: Via s. Antonio 14, 38100 Trento, Italy

EDUCATION

- Current pharmacy student at the Pharmacy University of Innsbruck enrolled in the 9th semester.
- High-School Diploma from the Franziskanergymnasium (Bozen, Italy) in July 2009 with the final of grade 82/100.
- Exchange High-School Semester at Mater Dei High School (Evansville, IN USA) in 2008 with a GPA of 3.92
- Middle school 2001-2004 at Scuola Media Bresadola (Trento, Italy) with the final grade of 100/100.
- Elementary school 1996-2001 at Scuola Elementare Crispi (Trento, Italy) with the final grade of 100/100.

INTERNSHIPS

- **Internship at E-Pharma** (Trento, Italy) in August 2011, working in a research lab to

provide quality check-ups of drugs in effervescent form and to validate new methods. I used analytic chemistry methods, HPLC, photometers. I also worked in the pharmaceutical technology lab. I assisted new development of optimal formulation for effervescent drugs. (see attachment with reference from E-Pharma)

- **Internship at Pharmacy “Bolghera” Trento** in February 2010. I worked in the lab preparing lotions, gels and capsules. I also helped out selling and providing the drugs for the patients.
- **Internship at Purdue University, West Lafayette, Indiana USA about radiopharmaceutical compound for tumor and heart imaging purposes.** I worked in a research environment testing radiopharmaceuticals in vivo to prove their efficacy. I gathered knowledge about SPECT scans and planar imaging procedures. I also learnt several handling, surgery and injection techniques on rodents.

WORKING EXPERIENCES

- **Professor’s Assistant in “Quantitative Inorganic Analysis Laboratory”** at the University of Innsbruck in May-June 2013. I advised the students during the analysis, prepared the analysis materials and corrected their analysis results. I was responsible for the experiments with the AAS (Atomic Absorption Spectroscopy) and FES (Flame Emission Spectroscopy).
- **Entertainer and project leader at English and German Summer Camps** of CLM Bell Language school of Trento during Summer 2012, 2011 and 2010. As a project leader I was in charge of organizing manual activities that would help the kids to learn new English

words. I had to coordinate the assistants so that they would work together to help the kids in the learning process.

- **Store assistant at Douglas Austria** in December 2011, 2012. I worked in a busy team providing a quality service to customers.
- **Junior leader in a CISV (children's international summer villages) summer camp** in the Philippines.
- **Head of the CISV Junior Section of Trento, Italy for the year 2010-11.** I was in charge of organizing the activities for the young people of the association, of maintaining the contact between the Section of Trento and CISV Italy. I also had to select the best people in my team that would get the chance to take part of international activities. We spent the year trying to help stop violence against women in our town and volunteered to help those who had had such a bad experience. I helped open a new section of CISV in Bosnia.

LANGUAGE SKILLS

- **Italian:** my mother language.
- **German:** I started studying German at the age of 11, at the age of 17 I passed the bilingual exam that recognizes the knowledge of Italian and German of level C1. I am currently studying in college in German.
- **English:** I started studying it when I was 6, the high-school year that I spent in the USA significantly improved my language skills. The foreign language certificates I have received are the PET (2006). My TOEFL score taken in October 2013 (West Lafayette, USA) is 106/120.